

Estimation of direct energy consumption and CO₂ emission by high speed rail, transrapid maglev and hyperloop passenger transport systems

Janić, Milan

DOI

[10.1080/15568318.2020.1789780](https://doi.org/10.1080/15568318.2020.1789780)

Publication date

2020

Document Version

Final published version

Published in

International Journal of Sustainable Transportation

Citation (APA)

Janić, M. (2020). Estimation of direct energy consumption and CO₂ emission by high speed rail, transrapid maglev and hyperloop passenger transport systems. *International Journal of Sustainable Transportation*, 15 (2021)(9), 696-717. <https://doi.org/10.1080/15568318.2020.1789780>

Important note

To cite this publication, please use the final published version (if applicable). Please check the document version above.

Copyright

Other than for strictly personal use, it is not permitted to download, forward or distribute the text or part of it, without the consent of the author(s) and/or copyright holder(s), unless the work is under an open content license such as Creative Commons.

Takedown policy

Please contact us and provide details if you believe this document breaches copyrights. We will remove access to the work immediately and investigate your claim.



Estimation of direct energy consumption and CO₂ emission by high speed rail, transrapid maglev and hyperloop passenger transport systems

Milan Janić

To cite this article: Milan Janić (2021) Estimation of direct energy consumption and CO₂ emission by high speed rail, transrapid maglev and hyperloop passenger transport systems, International Journal of Sustainable Transportation, 15:9, 696-717, DOI: [10.1080/15568318.2020.1789780](https://doi.org/10.1080/15568318.2020.1789780)

To link to this article: <https://doi.org/10.1080/15568318.2020.1789780>



© 2020 The Author(s). Published with license by Taylor & Francis Group, LLC



Published online: 15 Jul 2020.



[Submit your article to this journal](#)



Article views: 3946



[View related articles](#)



[View Crossmark data](#)



Citing articles: 6 [View citing articles](#)

Estimation of direct energy consumption and CO₂ emission by high speed rail, transrapid maglev and hyperloop passenger transport systems

Milan Janić

Department of Transport & Planning, Faculty of Civil Engineering and Geosciences, Delft University of Technology, Delft, The Netherlands

ABSTRACT

This paper deals with estimation of direct energy consumption and related emissions of GHG exclusively, including CO₂, by the High Speed Rail (HSR), Trans Rapid Maglev (TRM), and Hyperloop (HL) passenger transport systems. This includes developing the corresponding analytical models based on the mechanical energy and applying them according to the specified what-if operating scenarios. The analogous models are developed and applied to the Air Passenger Transport (APT) system for comparison purposes. The results of the application of the proposed models under given conditions have indicated that the average and total energy consumption and related emission of CO₂ of the three systems have been generally sensitive, i.e. elastic to variations of the nonstop journey distance and the vehicle/train seating capacity. Their average values have decreased more than proportionally and total values in proportion with increasing of the nonstop journey distance. Both have decreased with increasing of the vehicle/train seating capacity per departure. In the case of supplying equivalent equally utilized transport capacities, the HSR and the TRM have had lower energy consumption and related emission of CO₂ than the HL system. As well, the HSR, the TRM, and the HL have had lower energy consumption and related CO₂ emission than the selected APT aircraft up to some 'breaking' journey distance under given what-if operating scenarios.

ARTICLE HISTORY

Received 29 November 2019
Revised 26 June 2020
Accepted 26 June 2020

KEYWORDS

Analytical models; CO₂ emission; energy consumption; HL; HSR; mechanical energy; TRM; what-if scenarios

1. Introduction

Comparison of the existing and new transport systems has frequently been based on expressing their performances in absolute terms. As such, these performances have been presented to policy makers and the public in a 'promotional/marketing' manner rather than as strongly scientifically and professionally supported evidence. The outcomes have usually only indicated the 'strength' of one system over the other (Feigenbaum, 2013). The stronger scientific/professional approaches have included multi-criteria evaluations of the performance of these systems in addition to the frequently used Cost-Benefit-Analysis (CBA). This former has included weighting the selected performances of these systems, reflecting their relative importance for the particular actors/stakeholders involved, again under specific conditions. The latter has dealt with the evaluation of their economic and financial feasibility during the life-cycle (Hwang & Yoon, 1981; Janić, 2003, 2018; Vuchic & Casello, 2002). Consequently, the real 'strengths' and 'weaknesses' of the new systems have become clearer only after their implementation.

At present, three ground rail-based High Speed (HS) passenger transport systems¹ can be examples under the above-mentioned consideration. While the High Speed Rail (HSR) system has been implementing worldwide, the TransRapid Maglev (TRM) system is still operating at the very limited scale (Cassat & Bourquin, 2011; Janić, 2016). Nevertheless, most recently, the plans for wider implementation of the TRM system have been considered (<https://asia.nikkei.com/Business/Transportation/China-looks-to-build-new-maglev-rail-line-to-boost-economy>). The Hyperloop (HL) system, launched just in the abovementioned 'promotional/marketing' manner, is still at the conceptual stage, i.e. under preliminary investigation and limited experimentation (Decker et al., 2017; Van Goeverden et al., 2018; Musk, 2013; <https://ec.europa.eu/eipp/desktop/en/projects/project-9401.html>). Among others, the TRM and the HL systems have particularly claimed higher operating speeds and consequently shorter journey time compared to the HSR as the exclusive 'advantageous' performance for users/passengers. However, despite such claims, the most recent opinion of academics and professionals worldwide has indicated that, for example, while the TRM system may have some potential for wider

CONTACT Milan Janić  M.Janic@tudelft.nl milanjanic3@gmail.com  Department of Transport & Planning, Faculty of Civil Engineering and Geosciences, Delft University of Technology, Delft, 2628 BX, The Netherlands.

¹In this paper, ground rail-based systems are those whose vehicles run on dedicated ground-positioned guideways: the HS trains on tracks (rails or railroads), the TRM trains on dedicated guideways, and HL capsules/pads within vacuum tube.

© 2020 The Author(s). Published with license by Taylor & Francis Group, LLC

This is an Open Access article distributed under the terms of the Creative Commons Attribution-NonCommercial-NoDerivatives License (<http://creativecommons.org/licenses/by-nc-nd/4.0/>), which permits non-commercial re-use, distribution, and reproduction in any medium, provided the original work is properly cited, and is not altered, transformed, or built upon in any way.

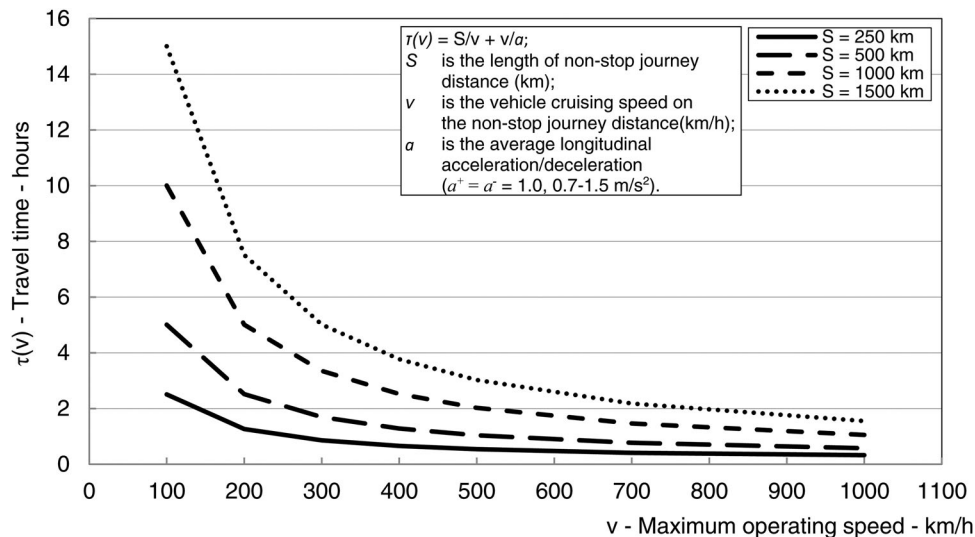


Figure 1. Examples of the relationships between the travel time, maximum operating speed, and nonstop journey distance.

implementation in the future, the HL system is not considered sufficiently promising, at least not for passenger transportation (Cassat & Bourquin, 2011; Wenk et al., 2018). Nevertheless, it has also been considered for possible operation in underwater tubes (Decker et al., 2017). This has again triggered the question of a fair comparison of the existing HSR, the still limited TRM, and the conceptual HL systems, according to the specified performances. Since operating at higher speeds generally requires higher energy consumption, this paper just aims to develop convenient generic models for estimating and comparing the energy consumption and related emissions of Green House Gases (GHG), particularly focused on Carbon Dioxide (CO_2), by these three systems. These models are applied to the operation of the three systems, according to the equivalent what-if scenario. This paper aims to generally fill a gap in existing knowledge on the abovementioned systems in the given context. As such it contains scientific and practical novelties as follows:

- The scientific novelty is represented by the generic analytical models developed for estimating direct energy consumption and CO_2 emission of the three HS rail-based electrically-powered transport systems. These models are exclusively based on mechanical energy. Thanks to such generality, they can be also applied to existing and new rail-based transport system using either technology and corresponding type of energy, such as diesel, hybrid (diesel/electric), hydrogen fuel, wind, and solar; and
- The practical novelty is represented by the case-specific application of these models to estimating and comparing direct energy consumption and CO_2 emission of the abovementioned existing (the HSR and partially the TRM) and eventually the forthcoming (HL) high-speed rail passenger transport systems operating according to the specified what-if scenario(s).

In addition to this introductory section, the paper consists of five other sections. Section 2 describes the relevance

of traveling at high speed for passengers and some relevant characteristics of the three considered HS systems. Section 3 provides an overview of literature and the main objectives of the paper. Section 4 presents the analytical models for estimating direct energy consumption and CO_2 emission according to the what-if operating scenario(s). Section 5 presents an application of the proposed models to hypothetical operating scenarios using input data taken from secondary sources. The last section summarizes some conclusions.

2. High speed rail-based passenger transport systems

2.1. Relevance of traveling at high speed

People have endeavored to increase travel speed for a long time. In general, the main driving forces for developing the abovementioned HS rail-based passenger transport systems have been limitations on travel time and monetary budget and maximizing distances in as short a time as possible, at a reasonable cost. Increasing travel speed has actually decreased the user/passenger travel time. The maximum operating speed of three considered HS systems have typically been 300–350 km/h (HSR), 400–500 km/h (TRM), and as much as 1,000–1,200 km/h (HL). However, it can be shown that increasing the operating speed generally marginally and differently contributes to savings in travel time, depending on the length of journey distance (Vuchic & Casello, 2002). Figure 1 shows an example of the relationships between travel time, operating speed, and journey distance.

As can be seen, for example, on a distance of 250 km, increasing of the operating speed from 100 to 200 km/h and from 200 to 300 km/h brings a saving in travel time of about 75 and 25 min, respectively. On the distance of 500 km, increasing of the operating speed from 300 to 500 km/h, 500 to 700 km/h, and 700 to 1,000 km/h, brings the savings in travel time of about 39, 16.2, and 7.5 min, respectively. On the distance of 1,500 km, these savings are 119, 50, and 37 min, respectively. This implies that the marginal increase

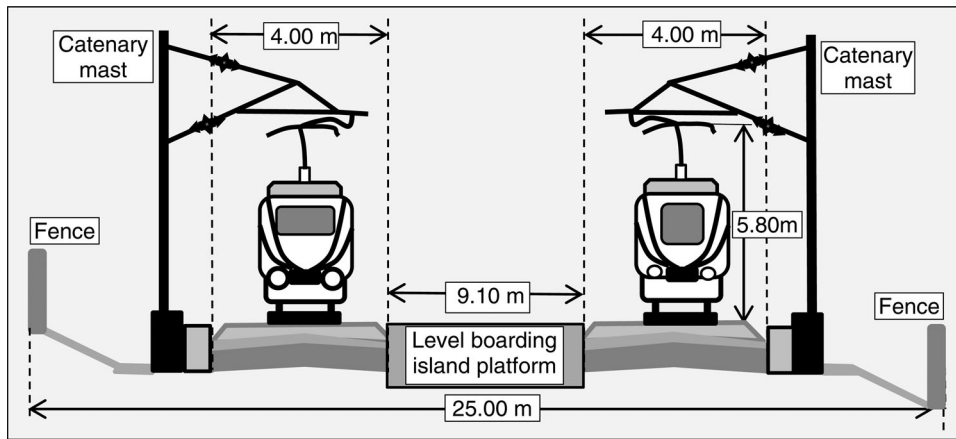


Figure 2. Scheme of the right-of-way of the HSR system at the stop/station (Janić, 2018).

in the operating speed on the given distance results in the disproportional decrease of marginal travel time gains. These gains are greater on greater distances. The presented figures again raise the issue of the relevance of gains in travel time on account of increasing the maximum operating speed on the one hand and the correspondingly increasing of energy consumption and related CO₂ emission on the other. Therefore, what are these like for the three HS rail-based systems?

2.2. High Speed Rail

The High Speed Rail (HSR) system has been developing worldwide (Europe, Far East-Asia) over the past sixty years as a rather innovative HS rail-based transport system (<https://uic.org/High-Speed-History>). Despite the common name, different definitions of this system have been used. In Japan, the HSR system called Shinkansen (i.e. the ‘new trunk line’) has operated trains at speeds of at least 200 km/h. The system’s network has been built with specific technical standards (i.e. dedicated tracks without level crossings and with standardized and special loading gauge). In Europe the HSR system, including compatibility of infrastructure and rolling stock, has enabled operation at speeds equal and/or greater than 250 km/h (Category I). In China, according to Order No. 34, 2013 by China’s Ministry of Railways, the HSR system refers to the newly-built dedicated lines with (actual or reserved) speeds equal and/or greater than 250 km/h (the specific acronym is CRH – China Railway High-speed). In the USA, the HSR system is considered as providing frequent express services at speeds of at least 150 mph, between the major population centers, at a distance of 200 to 600 miles, with few intermediate stops. These services must be provided on completely grade-separated, dedicated right-of-way lines (Campos & de Rus, 2009; EC, 1996, Janić, 2016; UIC, 2010a; Wendell & Vranich, 2008). Figure 2 shows the scheme of right-of-way of the HSR system at the stop/station (Janić, 2018).

The traction power for HS trains is provided by 15 kV/16.7 Hz or 25 kV/50 Hz AC systems. The traction power, contained in the traction converter, synchronized AC motors, and transformer at the front, along, and at the back

of the train, generally varies between 5.5 and 13.2 MW/train (<http://www.Trainweb.org/tgvpages/tgvindex.html>).

Additional characteristics of the HSR system are given below, as inputs of the models for estimating energy consumption and related CO₂ emission.

2.3. TRM (TransRapid Maglev)

The TRM (TransRapid MAGLEV – MAGnetic LEVitation) has been developing at the conceptual, experimental and limited operational scale for the past fifty years. The system is based on Herman Kemper’s idea of the magnetic levitation, dating from 1930s. The TRM system has been only fragmentary implemented, connecting airports and city centers. At the present, the TRM network at a larger scale, similarly as that of HSR, is far from development and implementation (Schach & Naumann, 2007; USDT, 2004; https://en.wikipedia.org/wiki/Shanghai_maglev_train; <https://www.travelchinaguide.com/cityguides/shanghai/getting-around.htm>). Figure 3 shows the scheme of right-of-way of the TRM system along the line/guideway (Janić, 2014).

The main technical characteristics of the TRM system are: i) levitation and guidance; ii) propulsion; and iii) power supply system (Cassat & Bourquin, 2011; Fritz et al., 2018; Wenk et al., 2018).

2.3.1. Levitation

The levitation of TRM train is based on two basic technologies: EMS (Electromagnetic Suspension) and EDS (Electrodynamical Suspension).

- EMS technology is based on the attractive properties of magnets. The first set of (electro) magnets (stator) is located on the underside of guideway (guidance rail) and the other on the undercarriage of train (levitation electromagnet). These two sets of electro magnets generate the upward electromagnetic force that enables the train to levitate at a certain (magnetic) air gap (usually ≤ 25 mm) (For the German TRM this gap is 10 mm). This force does not depend on the train’s speed and also exists at zero speed, i.e. while the train is stopped.

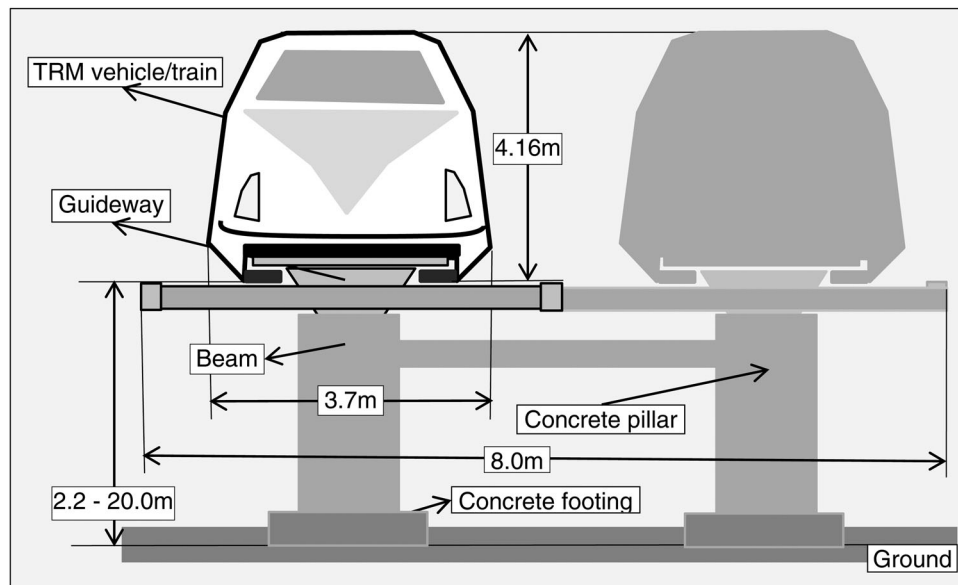


Figure 3. Scheme of the right-of-way of the TRM system along the line/guideway (Janić, 2014).

Additionally, the undercarriage (guiding) electromagnets generate the magnetic force that provides the lateral stability (guidance) of the train. This technology is used by the German/Chinese TRM (TransRapid) and urban (Japan HSST and Korean Incheon) systems.

- EDS technology is based on the electromagnetic induction. The train is equipped with superconducting magnets on each side, moving at a relatively high speed along the guideway equipped with a series of coils on each side. Moving at such high speed induces a current on the coils, exerting magnetic force on the superconducting magnets. This force levitates the train at the certain (magnetic) air gap, which is usually ≤ 80 mm, depending on the weight of train. Since the coils can induce current and generate magnetism only when the superconducting magnets are moving at high speed, the train cannot levitate at the speeds lower than 100 km/h, thus requiring wheels to operate.

2.3.2. Propulsion system

Short- and/or long-stator Linear Synchronous Motors (LSMs) or the rotating motors constitute the propulsion system of TRM system. In general, the LSM consists of two components: i) the stator underside of the guideway, producing a magnetic field along the guideway; and ii) the excitation system onboard the train, which stimulates the levitation electromagnets to produce an excitation magnetic field. After synchronizing and locking both magnetic fields, the generated propulsion force pulls forward and thrusts the train. At the same time, the induced magnetic resistance force opposes this propulsion force. Some estimates indicate that the resulting minimum mechanical power has been around 8 MW (Cassat & Bourquin, 2011).

2.3.3. Power supply system

The Power Supply (PS) system of 110 kV/50 Hz (or 154 kV/50–60Hz) provides the external energy supply to the TRM

system, including its propulsion system, onboard the train, the operations control system, guideway switches, and the reactive power compensation. The components of the PS system are installed at substations and transformer stations located along the line/guideway.

Additional characteristics of the TRM system are given below, as inputs of the models for estimating energy consumption and CO₂ emission.

2.4. Evacuated tube passenger transport systems

The idea about transportation of both passengers (and freight) through vacuum tubes aiming at increasing transport speed, but not necessarily the energy consumption due to increased air resistance, goes back a long way (<https://www.businessinsider.nl/history-hyperloop-pneumatic-tubes-a-s-transportation-2017-8/?international=true&r=US/>; http://www.railway-energy.org/static/Swissmetro_61.php; <https://ec.europa.eu/eipp/desktop/en/projects/project-9401.html>). In general, the idea has implied the deployment of levitating vehicles within the vacuum tubes. These would transport passengers and freight at high speeds, consequently substantially shortening their travel time compared to that of the existing modes (Janić, 2019). As such, these have been claimed not only as the new systems within existing ones, but also as completely new transport modes. In this paper, they are considered as some kind of rail-based system because of being based on the already existing ideas and relatively well-elaborated (known) technologies.

2.4.1. Swissmetro

The Swissmetro system was originally planned and designed as the HS transport system for connecting the Swiss metropolitan areas. Later on, labeled as Eurometro, it was also considered for connecting the main European cities (http://www.railway-energy.org/static/Swissmetro_61.php). The system would be based on magnetic levitation technology, with

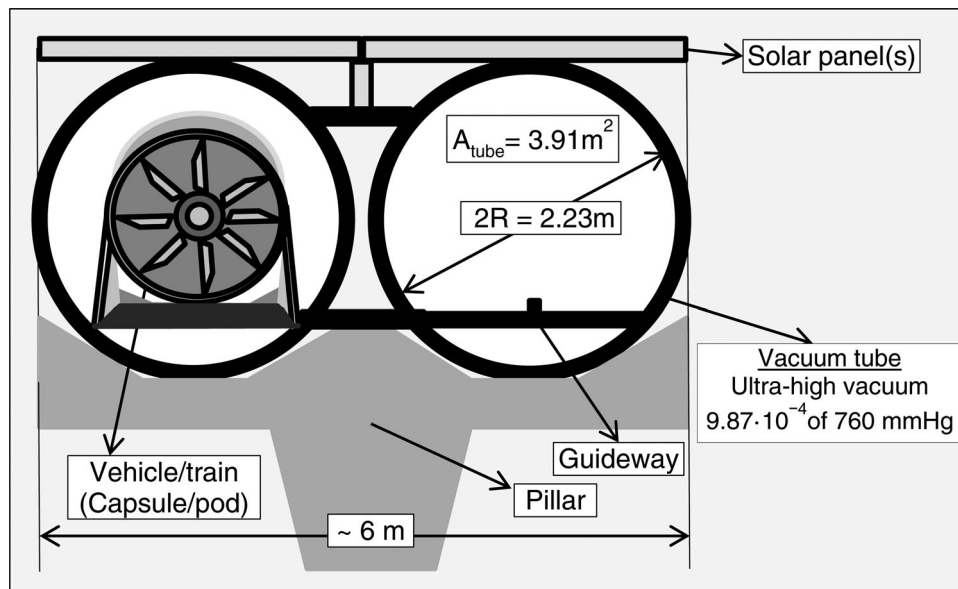


Figure 4. Scheme of the right-of-way of HL system along the line/tube (the “Hyperloop Passenger Capsule” version) (Janić, 2018; Musk, 2013).

vehicles operating within partially evacuated underground tubes at a maximum speed of 300–500 km/h. Initially, the length of the network of lines, each with two tubes, had been planned to be 411 km. The interior diameter of each tube, with a length of 60–300 m was 5 m. The air pressure within the tubes would be equivalent to that at the altitude of 15,000–18,000 m Mean Sea Level (MSL), i.e. 1,000–10,000 Pa or 0.01–0.1 atm. It had aimed to reduce the vehicle’s aerodynamic resistance when operating at high speed. The length of each vehicle was 80 m, an external diameter of 3.2 m, and with a capacity of 200 seats. The coupling of two or more vehicles had been also considered, for increasing single departure capacity to 400 and/or even 800 seats. The vehicles/trains would be propelled by linear electric motors and the magnetic levitation and guidance system (comparable to that of the TRM system). The vehicles would levitate 20 mm above the track/guideway. As such, compared to its HSR and TRM counterparts, this system was expected to provide higher service quality in terms of transport service frequency, seating capacity, shorter travel times thanks to the higher speed, lower energy consumption and consequently CO₂ emission, and complete lack of noise (Cassat et al., 2003; EPFL, 1993; Mossi & Rossel, 2001).

2.4.2. Hyperloop

The Hyperloop (HL) is the most recent HS passenger (and freight) transport system, proposed by Elon Musk in 2013. Still at the conceptual and very limited experimental stage, it has been claimed that it is superior to its HSR and TRM counterparts, offering higher operating speed, shorter travel time, and lower travel costs. However, this is still to be proven after the system’s eventual initial commercialization (Musk, 2013; Taylor et al., 2016; Wenk et al., 2018). The main components of the HL system are infrastructure, vehicles, and the supporting facilities and equipment. The infrastructure of the HL system consists of the vacuum tubes and stations. The tubes are steel, with the wall thickness of

2–3 cm and diameter of 2.23 m for the Hyperloop Passenger Capsule and 3.6 m for the Hyperloop Passenger Plus Vehicle Capsule version. The tubes, as guideways for the capsules, are positioned on raised pillars, approximately 30 m apart, with the exception of tunnel and bridge sections. The ultra-high vacuum maintained in these tubes would be 0.75 Torr (0.015 psi or 100 Pa) (British and German standards). Figure 4 shows the scheme of right-of-way of the Hyperloop Passenger Capsule version along the line (Chin et al., 2015; Janić, 2018; Musk, 2013; Taylor et al., 2016).

The HL system stations would consist of three modules integrated with the tube. The first is the ‘arrival’ vacuum chamber. After handling an arriving capsule, the chamber is de-vacuumed. Then, the capsule proceeds to the second module/chamber where normal atmospheric pressure prevails. This allows for passenger disembarkation and embarkation. Then, the capsule passes to the third (‘departure’) chamber where normal atmospheric pressure prevails. The capsule waits until the chamber is vacuumed, then leaves it, and proceeds through the tube. The modules/chambers are separated by the hermetic doors maintaining the required air pressure (Decker et al., 2017; Musk, 2013).

The system of LSMs would provide propulsion for the HL capsules. Each LSM consists of the rotor on the capsule and the stator with modules located along the tube at specified distances. These actually provide power, enabling the capsule to accelerate up to the cruising speed, maintain this speed through periodic boosts, and decelerate toward the end of journey. The periodic boosting of capsule requires the (electromagnetic) energy for overcoming its existing inertial despite the weak air resistance force during the journey. The levitation of the capsule requires the energy consumed for overcoming the corresponding force. This is approximately proportional to the capsule’s potential energy, depending on its weight and the levitation gap. The levitation force maintaining the capsule above the track can be provided either by TRM technology (see above) or an air bearing system. This latter is supported by the compressor

system consisting of an onboard compressor driven by an electric motor, powered by a battery pack. The onboard compressor primarily neutralizes a sharp increase in the aerodynamic drag force due to the air mass build-up in front of the capsule operating at speeds close to Mach 1 (Kantrowitz Limit) (At this speed, regardless of density, air tends to be compressible (Kantrowitz, 1947)). In addition, the compressor system also contributes to the acceleration of the capsule during its boosting by LSMs. It also pushes the pressurized air into the air bearing system below the capsule to support its levitation, increases the overall thrust at the very low scale, and feeds the auxiliary power. The most recent HL system would likely use Superconducting Magnetic Levitation (SML) technology, inducing almost or zero magnetic resistance force. The initial traction power for acceleration/deceleration of the capsule to/from the maximum operating speed, respectively, has been estimated to be around 46 MW (Chin et al., 2015; Decker et al., 2017; Musk, 2013).

The energy for operating the system (primary LSMs and battery packs supplying the compressor system on board) has initially been proposed to be obtained from solar panels located on top of the tubes (Figure 4). Alternatively, the energy from the conventional (electrical) power supply system can also be considered. Finally, the system's supporting facilities and equipment include the power supply system, vacuum pumps, and the traffic control/management system.

The additional relevant characteristics of the HL system are given below, as inputs of the models for estimating its energy consumption and CO₂ emission.

3. Literature overview and objectives of the research

There has been considerable research generally dealing with the performances of the HS transport systems. This research has generally dealt with analyzing the systems, their comparison, multi-criteria evaluation, and explicit analytical and simulation modeling and estimating their energy consumption and related GHG emissions. Some rather limited examples of analyses of these systems are related to the HSR system (Janić, 2016; UIC, 2010a, 2010b; Ziemke, 2010). Frequently, the performances of HS rail-based systems have implicitly and/or explicitly been compared with that of the Air Passenger Transport (APT) system, as the potential competitor on the short- to medium-haul distances (mainly the case in Europe) (Campos & de Rus, 2009; EC, 1996; Feigenbaum, 2013; Wendell & Vranich, 2008). A similar approach has been applied to analyzing the performances of the TRM system (Cassat & Bourquin, 2011; Janić, 2014). The illustrative cases of comparison of performances of have related to HSR and TRM (Schach & Naumann, 2007; Vuchic & Casello, 2002), as well as to the TRM and the HL systems (Taylor et al., 2016). Also, elaborating the vacuumed transport systems, both the Swissmetro and recently the HL system have mainly included descriptions of their infrastructural, technical/technological, operational, economic, environmental, and social advantages, compared to those of the

HSR and the TRM systems (Cassat et al., 2003; Chin et al., 2015; Decker et al., 2017; EPFL, 1993; Mossi & Rossel, 2001; Musk, 2013). In the abovementioned research, the energy consumption and related emissions of GHG have been considered as important indicators of performances, used as the criteria in the multi-criteria evaluation of these systems (Janić, 2018). The research estimating the energy consumption and related GHG emissions of the HSR and the TRM systems has also been substantial, using existing and developing new analytical and simulation models (Baker, 2014; Feng et al., 2014; UIC, 2010b; Wang & Sanders, 2012). In some other cases, only the results from calculations have been presented, without the corresponding methodological approach. The most recently published research dealing comparing the energy consumption of the TRM and the HSR is an illustration of such approach. In addition, the energy consumption of the HSR and the TRM has often been expressed with regard to the maximum operating speed, very often not or only indirectly mentioning the journey distances (Fritz et al., 2018). However, the analytical modeling and estimation of the energy consumption and CO₂ emission of the HL system and their comparison to that of the potential counterparts—the HSR, the TRM and also the APT—has been lacking.

This paper aims to fill this gap. Therefore, its main objective was to develop new generic analytical models for estimating direct energy consumption and related CO₂ emission of three HS systems: the HSR, the TRM, and the HL. They are assumed to operate according to the what-if scenarios, generally based on equivalent nonstop journey distances and supply of transport capacities.

4. Modeling energy consumption and CO₂ emission

4.1. General

In addition to land use, energy consumption and related GHG emissions can be considered the environmental performances of the three abovementioned HS rail-based systems. These are directly influenced by their technical/technological and operational performances, and indirectly by economic performance (Janić, 2016, 2018). In the given case, they are modeled as directly influenced by the technical/technological and operational performances.

4.2. Basic model

In the remaining part of the paper the term “vehicle/train” is used in order to achieve compatibility of the three systems. In railways, the running resistance of vehicles/trains to motion has been commonly used for estimating the required power to overcome it. In most cases, this resistance has been expressed by Davis' equation of the running resistance as follows (Davis, 1926; Schetz, 2001):

$$R = a + bv + cv^2 \quad (1)$$

where

- v is the vehicle/train speed; and
 a, b, c are the coefficients determined from theoretical consideration or measurement.
 c is the coefficient of aerodynamic resistance.

In Equation (1) coefficient (a) relates to the rolling resistance, coefficient (b) to the other mechanical resistance and drag associated with ingested air, and coefficient (c) to the aerodynamic resistance. In particular, the aerodynamic resistance of a given vehicle/train increases with the square of its speed, tending to dominate the overall resistance to motion, particularly at very high speeds. Consequently, numerous other variations, analytical, simulation, and empirical estimations of this basic equation, depending on the specific conditions, focus on estimating just the air resistance of HS trains (Peters, 1983; Schetz, 2001; UIC, 2010b).

4.3. Assumptions and scope of model development

The main assumptions and scope of development of the analytical models for estimating the energy consumption and related CO₂ emission of three HS rail-based systems are as follows.

- The direct energy consumption and related CO₂ emission of the three HS systems, operating according to the specified what-if scenarios, are considered exclusively. This implies that the Life Cycle Assessment (LCA) is not applied, i.e. building and maintaining infrastructure, manufacturing and maintaining rolling stocks, supporting facilities and equipment is not taken into account. One of the reasons for omitting the LCA is due to the fact that these systems, assumed to operate according to the specified scenarios, would use electricity obtained from the same primary sources. Consequently, this would produce the same effect when comparing them (Janić, 2018; UIC, 2010b).
- The principles of mechanical energy are exclusively applied, implying consideration of only the mechanical forces acting on the vehicles/trains of three systems during the journey. On the one hand, an exception is the consideration of the induced magnetic resistance force acting on TRM vehicles/trains using EMS and/or EDS levitation technology. On the other hand, this is assumed to be near-zero in the case of their HL counterpart using SML technology. The driving processes along the line(s) and behavior of their electrical sub-systems are not elaborated for three systems in detail. Such simplifications are made bearing in mind the availability of comparable relevant data, which would enable fair treatment of the three systems. However, this simplification is not expected to compromise the quality and relevance of the final results.
- The lines/guideways of the three systems are assumed to start and end at the same origin and destination terminals. The passenger access and egress time at these train/vehicle embarking/disembarking locations by the chosen (urban) transport mode would be approximately the same, thus making this component of energy consumption and related CO₂ emission irrelevant in the given

context. In addition, the stop-to-stop or terminal-to-terminal vehicle/train and not the door-to-door passenger journeys are considered exclusively.

- The specified what-if scenarios imply that the vehicle/trains operate at constant average acceleration/deceleration rates and cruising speeds along the given nonstop journey distances/lines without intermediate stops. Consequently, the impact of head and crosswind on the HSR and TRM vehicles/trains is not taken into consideration. Figure 5 shows the assumed speed profile (Feng et al., 2014).
- The HL system is assumed to be fully operational as specified in the elaboration of its concept.
- The estimated energy consumption and related CO₂ emission of the three systems are expressed in both relative and absolute terms, depending on the vehicle/train seating capacity, load factor, and the nonstop journey distance. In the former case they are expressed per unit of input/output (quantity/s-km). In the latter case they are expressed by the quantities per nonstop journey (quantity/journey). APT values are also provided for the comparative purposes.

4.4. Model structures

4.4.1. Single vehicle/train

As mentioned above, the models of direct energy consumption and related CO₂ emission are exclusively based on the mechanical forces acting on the HSR, the TRM, and/or the HL vehicle/train operating according to the specified what-if scenarios shown in Figure 6(a, b).

Figure 6(a) shows the inertial, aerodynamic, rolling, and gradient resistance force acting on the HSR vehicle/train. Figure 6(b) shows the inertial, aerodynamic, gradient, levitation, and induced magnetic resistance force acting on the TRM and the HL vehicle/train. The vehicles/trains of all three systems are also (but mainly theoretically) exposed to the aerodynamic lift force, particularly during cruising at maximum operating speed. This force is very weak in the case of the HSR and the TRM and does not exist in the case of HL vehicles/trains, due to it operating in a vacuum tube. Under such conditions, the total energy taken from the power supply system by a single vehicle/train, operating along the given nonstop journey distance in the single direction generally, consists of the energy consumed 'at wheel' and due to the auxiliary power supply. This total energy can be estimated as follows (Feng et al., 2014; Jong & Chang, 2005; Rochard & Schmidt, 2000; Zhou, 2014):

$$e_T(S) = e_W(S) + e_P(S) \quad (\text{kWh}) \quad (2a)$$

where

$$e_W(S) = (1/\eta_W) \cdot [e(s_a) + e(S - s_a - s_d) + e(s_d)] \cdot \varepsilon + k_0 e_v(S) \quad (\text{kWh}) \quad (2b)$$

where

$$s_a = v_c^2 / (2 \cdot a^+) \quad \text{and} \quad s_d = v_c^2 / (2 \cdot a^-) \quad (2c)$$

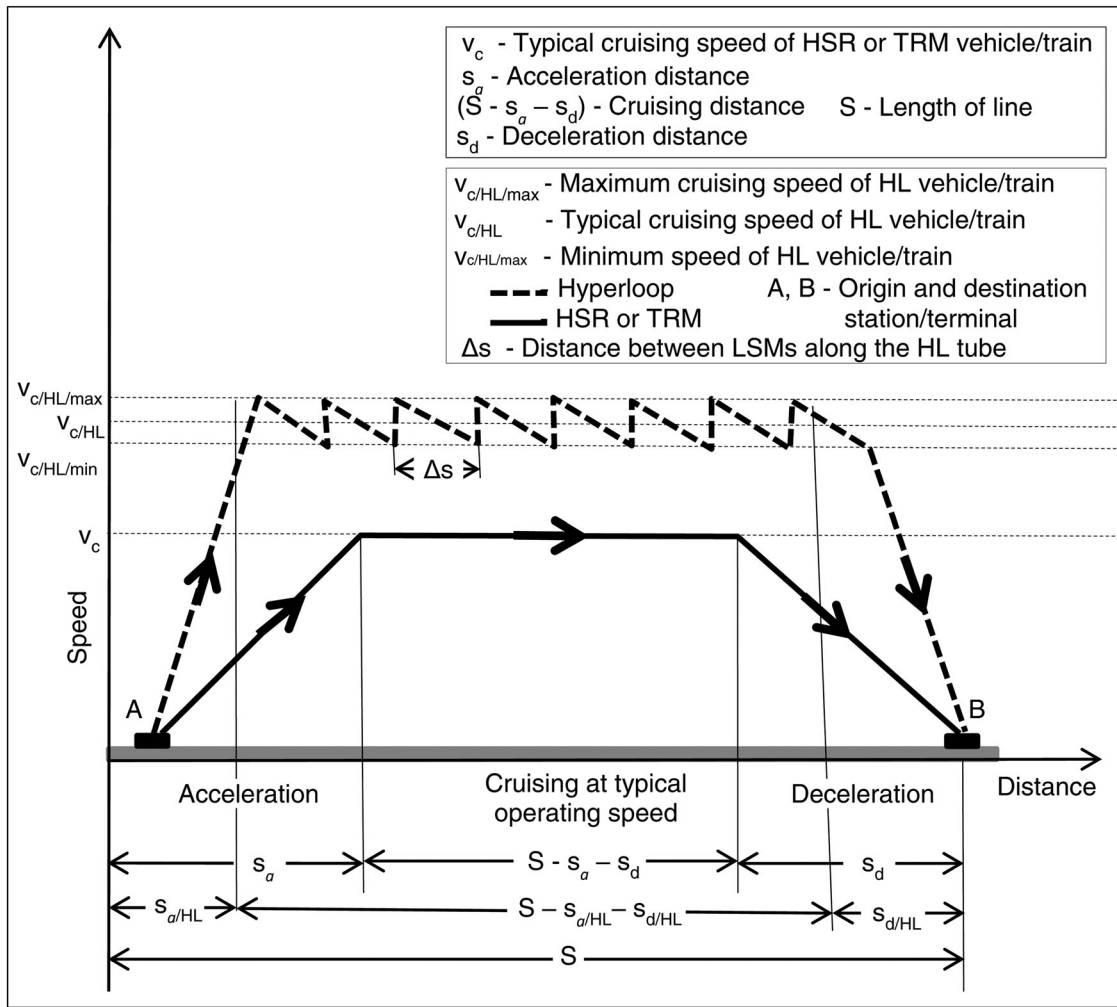


Figure 5. Scheme of the speed profile of the HS vehicles/trains operating along the nonstop journey distance used for estimating the energy consumption and emissions of CO₂.

In addition:

$$\begin{aligned}
 e_p(S) &= (1/\eta_{aps}) \cdot P_{aps} \cdot t(S) \\
 &= (1/\eta_{aps}) \cdot P_{aps} \cdot \left(\frac{1}{2} \frac{v_c}{a^+} + \frac{S}{v_c} + \frac{1}{2} \frac{v_c}{a^-} \right) \quad (2d)
 \end{aligned}$$

- $t(S)$ is the journey time along the nonstop journey distance (S) (h, min);
- P_{aps} is the auxiliary power supply (kW);
- η_{aps} is the efficiency of the auxiliary power supply system (-);
- v_c is the average cruising speed of the vehicle/train (m/s);
- ϵ is the conversion factor (J vs kWh) ($1 \text{ J} = 2.77778 \cdot 10^{-7} \text{ kWh}$); and
- J is Joule ($\text{kg} \cdot \text{m}^2/\text{s}^2$).

where

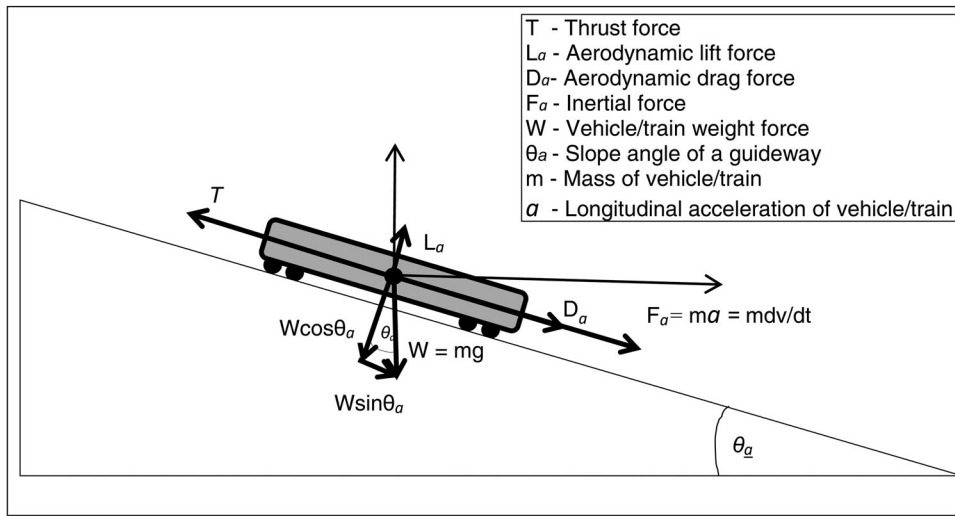
- $e_w(S)$ is the energy consumed 'at wheel' (kWh);
- $e_p(S)$ is the energy consumed for the auxiliary power supply (kWh);
- S is the nonstop journey distance (between two stops) (km);
- η_w is the overall efficiency of the HS system's traction system ('at wheel', onboard the vehicle/train, and power supply system) ($\eta_w \leq 1.0$);
- s_a, s_d are the average acceleration and deceleration distance of the vehicle/train, respectively (km);
- a^+, a^- are the average longitudinal acceleration and deceleration of the vehicle/train, respectively (m/s^2);
- $e(s_a), e(s_d)$ are the energy consumptions of vehicle/train during its acceleration and deceleration, respectively (J);
- $e(S-s_a-s_d)$ is the energy consumption of the vehicle/train during the cruising phase of the journey (J);
- k_0 is a binary variable taking the value '1' if the energy is consumed to support direct operation of the vehicle/train, and the value '0' otherwise ($k_0 = 1$ for HL and $k_0 = 0$ for HSR and TRM);
- $e_v(S)$ is the energy consumption for supporting direct operations of the vehicle/train (in this case for establishing and maintaining vacuum in the HL tube) (kWh);

The components of energy consumption in Equation (2b) can be estimated as follows:

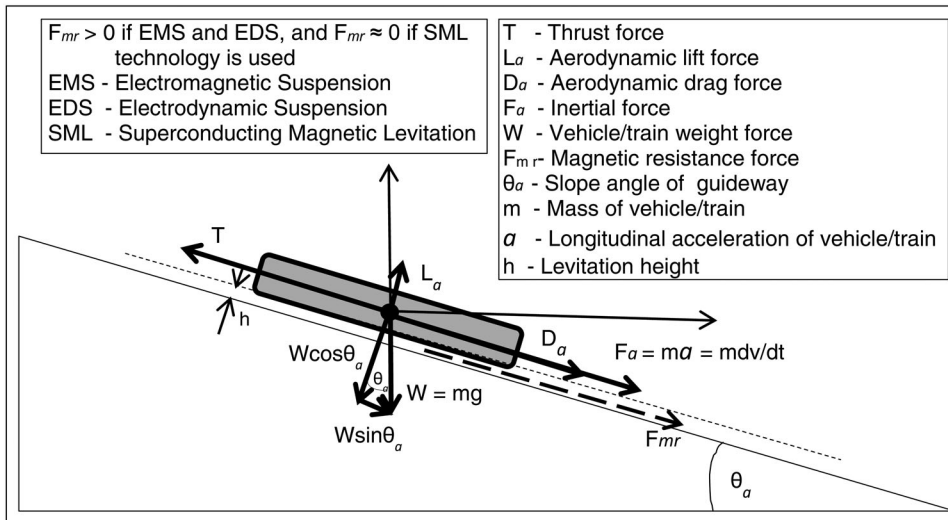
4.4.1.1. Acceleration.

$$\begin{aligned}
 e(d_a) &= \{ma^+ + D_a + W\sin\theta_a + k_1[\mu_R(W\cos\theta_a - L_a)]\}s_a \\
 &\quad + k_2[(W\cos\theta_a - L_a)h + k_4F_{mr/a}s_a] + k_3\{P_{cs}[\alpha(\bar{v}_a/c) \\
 &\quad + \beta](v_c/a^+)\} = \{ma^+ + 0.5\rho\bar{v}_a^2C_D A + mg\sin\theta_a \\
 &\quad + k_1[\mu_R(mg\cos\theta_a - 0.5\rho\bar{v}_a^2C_L A_1)]\}s_a \\
 &\quad + k_2[(mg\cos\theta_a - 0.5\rho\bar{v}_a^2C_L A_1)h \\
 &\quad + k_4F_{mr/a}s_a] + k_3\{P_{cs}[\alpha(\bar{v}_a/c) + \beta](v_c/a^+)\}
 \end{aligned} \quad (3a)$$

(continued)



a) HSR



b) TRM and HL

Figure 6. Scheme of the main forces acting on the HS (High Speed) vehicle/train during acceleration phase of the nonstop journey. a) HSR b) TRM and HL.

4.4.1.2. Cruising.

$$\begin{aligned}
 e(S - s_a - s_d) &= \{D_c + W\sin\theta_c + k_1 \\
 &\quad [\mu_R(W\cos\theta_c - L_c)]\}(S - s_a - s_d) \\
 &\quad + k_2\{(W\cos\theta_c - L_c)h + n[m(v_{c/\max} \\
 &\quad - v_{c/\min})^2/2] + k_4F_{mr/c}(S - s_a - s_d)\} \\
 &\quad + k_3\{P_{cs}[\alpha(v_c/c) + \beta] [(S - s_a - s_d)/v_c]\} \\
 &= \{0.5\rho v_c^2 C_D A + mg\sin\theta_c + k_1 \\
 &\quad [\mu_R(mg\cos\theta_c - 0.5\rho v_c^2 C_L A_1)]\} \\
 &\quad (S - s_a - s_d) + k_2\{(mg\cos\theta_c - 0.5\rho v_c^2 \\
 &\quad C_L A_1)h + [nm(v_{c/\max} - v_{c/\min})^2/2] \\
 &\quad + k_4F_{mr/c}(S - s_a - s_d)\} + k_3\{P_{cs} \\
 &\quad [\alpha(v_c/c) + \beta] [(S - s_a - s_d)/v_c]\}
 \end{aligned} \quad (3b)$$

The number of boosts (n) of the HL train/vehicle by LSMs during the cruising phase of journey in Equation (3b) is estimated as follows: $n = S/\Delta s - 1$.

4.4.1.3. Deceleration.

$$\begin{aligned}
 e(s_d) &= (1 - p_{reg})\{ma^- - D_d - W\sin\theta_d \\
 &\quad - k_1[\mu_R(W\cos\theta_d - L_d)]\}s_d \\
 &\quad + k_2[(W\cos\theta_d - L_d)h + k_4F_{mr/d}s_d] \\
 &\quad + k_3\{P_{cs}[\alpha(\bar{v}_d/c) + \beta](v_c/a^-)\} \\
 &= (1 - p_{reg})\{ma^- - 0.5\rho\bar{v}_d^2 C_D A - mg\sin \\
 &\quad \theta_d - k_1[\mu_R(mg\cos\theta_d - 0.5\rho\bar{v}_d^2 C_L A_1)]\} \\
 &\quad s_d + k_2[(mg\cos\theta_d - 0.5\rho\bar{v}_d^2 C_L A_1)h + k_4F_{mr/d}s_d] \\
 &\quad + k_3\{P_{cs}[\alpha(\bar{v}_d/c) + \beta](v_c/a^-)\}
 \end{aligned} \quad (3c)$$

In Equations (3a) (3b) and (3c), the magnetic resistance force of the TRM vehicle/train based on the EMS levitation technology can be estimated as follows:

$$F_{mrj} = \left\{ N_s \cdot \left(\frac{P_{LG} \cdot 3.6}{v} - 0.2 \right) + N_s \cdot \left[0.1 \cdot \sqrt{\frac{v}{3.6}} + 0.02 \cdot \left(\frac{v}{3.6} \right)^{0.7} \right] \right\} / 1000 \quad (3d)$$

4.4.1.4. Supporting direct operations of the vehicle/train (vacuum pumps in the HL system). The energy consumption ($e_v(S)$) in Equation (2b), for establishing and maintaining vacuum by the vacuum pumps in the HL tubes during the system's operating time, is estimated as follows (Decker et al., 2017):

$$\begin{aligned} e_v(S) &= \delta \cdot e_1(V) + e_2(V) \\ &= \delta \cdot \left[\frac{M \cdot Q \cdot (p_0 - p_r)}{36\eta_{vp}} \right] \cdot \left(\frac{V}{M \cdot Q} \right) \cdot \ln \frac{p_0}{p_r} \\ &\quad + \left[\frac{M \cdot Q \cdot (p_0 - p_r)}{36\eta_{vp}} \right] \cdot \Delta\tau \\ &= \delta \cdot \left[\frac{(p_0 - p_r) \cdot \pi R^2 \cdot S}{36\eta_{vp}} \right] \cdot \ln \frac{p_0}{p_r} + \left[\frac{M \cdot Q \cdot (p_l - p_r)}{36\eta_{vp}} \right] \cdot \Delta\tau \end{aligned} \quad (3e)$$

The required capacity of the vacuum pumps in the HL system (Q) in Equation (3e) is estimated as follows:

$$Q = V/\tau_p \quad (3f)$$

where

M	is the gross mass of the vehicle/train, including its empty mass and payload (i.e. passengers) (kg);
g	is the gravitational constant (m/s^2);
W	is the weight of vehicle/train ($W = mg$) (kp);
\bar{v}_a, \bar{v}_d	are the average speeds of the vehicle/train during acceleration and deceleration, respectively ($\bar{v}_a = v_c/2, \bar{v}_d = v_c/2$) (m/s);
$v_{c,max}, v_{c,min}$	are the maximum and minimum operating cruising speeds of the HL vehicle/train, respectively (m/s);
n	is the number of boosts of the HL vehicle/train by LSMs during the journey;
c	is the speed of sound under conditions close to that in the HL vacuum tube (334 m/s or 1238 km/h at the sea level);
μ_R	is the coefficient of rolling (friction) resistance (-);
C_L, C_D	are the coefficients of aerodynamic lift and drag, respectively (-);
ρ	is the air density (kg/m^3);
A	is the frontal area of vehicle/train (m^2);
A_l	is the lift area of vehicle/train (m^2);
$\theta_a, \theta_c, \theta_d$	are the longitudinal gradient angles of the guideway (or HL tube) segments where the vehicle/train perform acceleration, cruising, and deceleration, respectively ($^\circ$);
h	is the levitation gap of the TRM and/or the HL vehicle/train (mm); and
$F_{mr/a}, F_{mr/c}, F_{mr/d}$	

(continued)

p_{reg}	are the induced magnetic resistance forces during acceleration, cruising, and deceleration, of the TRM or the HL vehicle/train, respectively (N);
k_1, k_2, k_3	is the proportion of energy regenerated during deceleration, i.e. regenerative braking, of the vehicle/train (-);
k_4	are binary variables taking the value '1' if the vehicle/train is HSR, TRM, and HL, respectively, and the value '0' otherwise;
$e_1(V), e_2(V)$	is a binary variable taking the value '1' if EDS or EMS levitation, and the value '0' if SML technology is used;
V	are the energies consumed by the vacuum pumps for establishing and maintaining vacuum in the HL tube, respectively (kWh);
δ	is the volume of HL tube to be vacuumed (m^3);
M	is a binary variable taking the value '1' if the energy consumption for establishing the vacuum in the HL tube is taken into account, and the value '0' otherwise;
Q	is the number of vacuum pumps in the HL system (-);
R, S	is the capacity of the vacuum pump (m^3/h);
p_{cs}	are the radius and length of the HL tube, respectively (m);
α, β	is the power of the compressor system onboard the HL vehicle/train (kW);
η_{vp}	are the empirically estimated coefficients;
p_i, p_r	is the efficiency of the HL vacuum pumps (-);
p_l	are the initial and required pressure in the HL tube (N/m^2);
$\Delta\tau$	is the pressure in the HL tube after common leakage of the required vacuum (N/m^2);
N_s	is the reference operational time of the vacuum pumps maintaining a given pressure/vacuum in the HL tube (h);
v	is the number of sections/cars per vehicle/train;
P_{LG}	is the speed of vehicle/train (km/h);
Δs	is the power of the linear generator per vehicle/train section (kW).
τ_p	is the distance between LSMs within the HL tube (km); and
	is the time for vacuuming the HL tube specified in advance (h).

The other symbols are analogous to those in the previous equations.

The term in the first curly brackets of Equation (3a) represents the energy for overcoming the inertial force during constant acceleration up to the cruising speed, the aerodynamic drag force, the gradient force (the component of the vehicle/train weight parallel to the ground), and the difference between the weight and the lift force of the vehicle/train materializing as the rolling friction force (case of HSR where $k_1 = 1; k_2 = k_3 = 0$). The sign of these three forces depends on moving the vehicle/train uphill (+) or downhill (-). The term in the second curly brackets represents the energy for overcoming the levitation and the induced magnetic resistance force ($k_2 = 1; k_1 = k_3 = 0; k_4 = 1$ for TRM and $k_4 = 0$ for HL system). The term in the third curly brackets represents the energy consumed by the compressor system of HL vehicle/train. This is expressed as the product of its required power depending of the average vehicle/train speed and time for acceleration ($k_3 = 1; k_1 = k_2 = 0$). The sum of the abovementioned terms gives the consumed energy during the acceleration phase of journey.

In Equation (3b) the vehicle/train is assumed to cruise at constant speed. Thus, the term in the first curly brackets

represents the energy for overcoming the aerodynamic resistance force, a component of the vehicle/train weight force parallel to the ground, and the force as the difference between the vehicle train weight and the lift force materializing as the rolling (friction) resistance (case of HSR: $k_1 = 1$; $k_2 = k_3 = 0$). The sign of these forces depends on moving the vehicle/train uphill (+) or downhill (-). The term in the second curly brackets represents the energy consumed for overcoming the levitating and the induced magnetic resistance forces ($k_2 = 1$; $k_1 = k_3 = 0$; $k_4 = 1$ for TRM and $k_4 = 0$ for HL system)). Specifically, the sixth term represents the energy consumed by LSMs periodically boosting the HL vehicle/train to maintain cruising speed during the journey (see Figure 5). The term in the third curly brackets represents the energy consumed by the compressor system and levitation of the HL vehicle/train during cruising. This energy again depends on the required power influenced by the cruising speed and the energy for overcoming the magnetic drag force ($k_3 = 1$; $k_1 = k_2 = 0$). Summing up these terms yields the total energy consumed during the cruising phase of the journey.

In Equation (3c), the first term in the round brackets represents the portion of energy dissipated by pneumatic brakes or any other kind of braking. The rest is regenerated and returned to the power system. The term in the first curly brackets represents the energy for overcoming the inertial force during the constant deceleration from the cruising speed, the aerodynamic resistance force, with the negative sign indicating its contribution to deceleration, the component of the vehicle/train weight parallel to the ground, and the rolling (friction) resistance ($k_1 = 1$; $k_2 = k_3 = 0$). The sign of these three forces depends on moving the vehicle/train uphill (-) or downhill (+). The term in the second curly brackets represents the energy for overcoming the induced magnetic resistance and levitation force ($k_2 = 1$; $k_1 = k_3 = 0$; $k_4 = 1$ for TRM, and $k_4 = 0$ for HL system). The term in the last curly brackets represents the energy consumed by the compressor system of the HL vehicle/train during deceleration, i.e. depends on its required power, dependent on the average speed ($k_3 = 1$; $k_1 = k_2 = 0$).

In addition, Equation (3e) indicates that the vacuum pumps consume energy for establishing and maintaining the vacuum in the HL tube. Equation (3e) indicates that the capacity of vacuum pumps increases with the volume of the tube (depending on its length and diameter in the case of HL) and the specified vacuuming time. This implies that given the volume of the tube, a longer setup time will require the lower vacuum pump capacity, and vice versa. As can be intuitively expected, the consumed energy in both cases will be approximately the same. After an initial establishing the required vacuum, the vacuum pumps continue to maintain it in order to compensate its possible leakage (Decker et al., 2017).

4.4.2. Transport capacity on the line/route

From Equations (2a) (3a) (3b) and (3c), the total energy consumption by the total transport capacity supplied on the line/route during time (Δt) is estimated as follows:

$$E_{TOT}(\Delta t, S) = f(\Delta t, S) \cdot e_T(S) \quad (4a)$$

From Equation (4a), the corresponding CO₂ emissions during time (Δt) are estimated as follows:

$$EM_{GHG}(\Delta t, S) = E_{TOT}(\Delta t, S) \cdot r_{CO_2e} \quad (4b)$$

From Equation (4a) the average energy consumption by the supplied transport capacity during time (Δt) is equal to:

$$E_{AVG}(\Delta t, S, PL) = E_{TOT}(\Delta t, S) / [f(\Delta t, S) \cdot PL \cdot S] \quad (4c)$$

From Equation (4b) the average CO₂ emission during time (Δt) is estimated as follows:

$$EM_{AVG}(\Delta t, S, PL) = EM_{GHG}(\Delta t, S) / [f(\Delta t, S) \cdot PL \cdot S] \quad (4d)$$

where

$f(\Delta t, S)$ is the number of departures of vehicles/trains scheduled on the nonstop journey distance (S) during time (Δt) (dep/unit of time);
 PL is the seating capacity of vehicle/train (seats/veh); and
 r_{CO_2e} is the CO₂ emission rate (kg/kWh).

The other symbols are analogous to those in the previous equations.

5. An application of the proposed models

5.1. Inputs

The input data for the application of the abovementioned models represents some elements of the what-if operating scenarios of the three systems. These are the specific characteristics of vehicles/trains, the range of their nonstop journey distances, transport service frequencies and corresponding transport capacities, and some external conditions.

The available data on the relevant characteristics of the HSR, the TRM, and the HL vehicles/trains are taken from the different secondary sources. This data was inherently heterogeneous regarding the level of details and quality for the purpose. This is mainly due to being obtained from real-life operations (HSR), test experiments and limited operations (TRM), and elaboration of the concept (HL), all in combination with expert judgements. Consequently, in order to enable fair comparison of three systems, their typical average values/estimates, are given in the self-explanatory Tables 1, 2, and 3, respectively.

As can be seen, the typical configuration of the vehicles/trains is characterized by the number of cars and their gross mass, the latter based on load factor of $\lambda = 1.0$ (or 100%) (Chin et al., 2015; Janić, 2016, 2018). In addition, their cruising speeds are assumed to be the typical operating rather than maximum, thus closer reflecting reality. The same applies to the average acceleration/deceleration rates, guaranteeing the necessary riding comfort for passengers during all phases of the journey. In the cases of the HSR and the TRM vehicles/trains, the lift coefficient and corresponding lift force are assumed to be zero. This is a reasonable assumption due to requiring the rather stable operation

Table 1. Input data - HSR (High Speed Rail).

Characteristic/variable/parameter	Notation/dimension	Value
Carriages per vehicle/train ^a	–	12 ^h ; 20 ⁱ ; 10 ^j
Length ^a	l (m)	238 ^h ; 394 ⁱ ; 201 ^j
Width (average) ^a	w (m)	3.00
Height (average) ^a	H (m)	3.08
Frontal area (average) ^b	A (m ²)	11.5
Gross (total) mass ^a	m (tons)	484 ^h ; 752 ⁱ ; 435 ^j
Capacity ^a	PL (seats)	485 ^h ; 794 ⁱ ; 430 ^j
Load factor	λ (-)	1.0; 0.7; 0.5
Acceleration/deceleration (maximum) ^a	a^+ / a^- (m/s ²)	0.7/1.0
Typical average cruising speed ^a	v (km/h)	300 ^h ; 300 ⁱ ; 330 ^j
Air density	ρ (kg/m ³)	1.225
Coefficient of aerodynamic drag (average) ^b	C_D (-)	1.66
Coefficient of aerodynamic lift ^c	C_L (-)	~ 0.0
Longitudinal guideway angles ^d	$\theta_a, \theta_c, \theta_d$ (°)	0.23, 0.23, 0.23
Overall efficiency of the traction system ^d	η_W (-)	0.85
Coefficient of rolling resistance ^e	μ_R (-)	0.002
Auxiliary power supply ^f	P_{aps} (kW)	275
Efficiency of auxiliary power ^f	η_{aps} (-)	0.85
Proportion of the regenerative energy ^f	p_{reg} (-)	0.70
Transport service frequency ^g	f (dep/h/line)	12

^aWendell and Vranich (2008); http://en.wikipedia.org/wiki/ICE_3; <http://www.trainweb.org/tgvpages/tgvindex.html>

^bSocket (1996); Schetz (2001); Baker (2014);

^cNot relevant due to providing stability of the vehicle/train (Peters, 1983);

^dZiemke (2010);

^eMagel (2017);

^fZhou (2014); Witt and Herzberg (2008);

^gTypically advertised (Van Goeverden et al., 2018).

^hTGV Atlantique;

ⁱEurostar;

^jICE 3M - Including two power cars);

of vehicles/trains along the line/guideway, independently on their cruising speed and the impact of head and/or cross-wind. Because of operating in a vacuum tube, the lift coefficient and corresponding force of the HL vehicle/train is practically non-existent. The longitudinal guideway angles are assumed to be very small and far below the maximally allowed. These imply that the lines/guideways of all the systems are just straight in both vertical and horizontal plane, i.e. with a very large vertical and horizontal radius. The three systems are considered to operate along the short- to medium-haul nonstop journey distances of: $S = 100\text{--}1,200$ km. The energy consumption by the vacuum pumps of the HL tube is also taken into account. Because in practice the tube is never absolutely air tight during the regular operations, it is likely that the vacuum is going to leak particularly during the loading of the vehicles/trains into the tube. Consequently, the vacuum pumps are assumed to operate almost all the time, in order to maintain the required vacuum in tube. This makes the HL vehicles/trains available to operate continuously and thus being comparable to the other two systems. The same also applies to the compressor system onboard the HL train/vehicle. Last but not least, as mentioned above, despite the initial idea that the HL system use solar panels as the primary source of the required electrical energy, it is believed to be unrealistic in many cases (Musk, 2013). This is due to the uncertainty in the sufficient number of sunny days/hours for accumulation of the required energy for the system's reliable operation. Therefore, for fair comparison of the three systems, CO₂ emissions by the three systems, assumed to operate in Europe, are estimated based on the average rate from the

electricity production $r_{CO_2e} = 0.546$ kgCO₂/kWh (Agora Energiewende & Sandbag, 2018; WNA, 2011).

The transport service frequencies are set up at two levels: a) Single departure of the vehicle/train of each system during the given time; and b) multiple departures by the three systems supplying the equivalent transport capacity during the given time. Therefore, regarding the seating capacity of the HSR, the TRM, the and HL vehicle/train in Tables 1, 2 and 3, in addition to the single departure frequency (Case a), their equivalent supply of seating capacity is set up as follows: $28 f_{HL}$ (28 seats) $\approx 1f_{HSR}$ (794 seats) (Eurostar) and $25 f_{HL}$ (28 seats) $\approx 1f_{TRM}$ (696 seats) (Case b). For the purpose of comparison, some necessary input data for estimating the energy consumption and CO₂ emission by Air Passenger Transport aircraft with seating capacity comparable to that of the three HS rail-based systems, operating on short- and medium-haul distances/routes, are given in Table 4.

As can be seen, two aircraft types have different maximum Take-Off Weight (TOW), seating capacity, operating performances, and corresponding fuel consumption during the flight and LTO cycle.² Burning Jet A fuel produces a range of GHGs, the most voluminous of which is CO₂, i.e. $r_{CO_2e} = 3.16$ kgCO₂/kg of fuel or $r_{CO_2e} = 0.266$ kgCO₂/kWh (ICAO, 2011). Regarding the aircraft seating capacity and the HL vehicle/train in Table 3, in addition to the single departure frequency (Case (a), the equivalent transport capacities are set up as follows: $7 f_{HL}$ (28 seats) $\approx 1f_{APT}$ (189

²This is time of the aircraft approach, landing, taxiing-in, taxiing out, and take-off from the airport (ICAO, 2011).

Table 2. Input data - TRM (TransRapid Maglev).

Characteristic/variable/parameter	Notation/dimension	Value
Carriages per vehicle/train ^a	–	6
Length ^a	l (m)	153.06
Width ^a	w (m)	3.70
Height ^a	H (m)	4.16
Frontal area	A (m ²)	15.4
Gross (total) mass ^a	m (tons)	382–399
Capacity ^a	PL (seats)	472–696
Load factor	λ (-)	1.0; 0.7; 0.5
Acceleration/deceleration (maximum)	a^+/a^- (m/s ²)	0.7/1.0
Typical average cruising speed ^c	v (km/h)	450
Levitation height (vertical air gap) ^b	h (mm)	10
Air density	ρ (kg/m ³)	1.225
Coefficient of the aerodynamic drag ^d	C_D (-)	0.6
Coefficient of the aerodynamic lift ^e	C_L (-)	~ 0.0
Longitudinal guideway angles ^f	$\theta_{ar}, \theta_{cr}, \theta_d$ (°)	0.51, 0.51, 0.51
Overall efficiency of the traction system ^f	η_w (-)	0.75
Auxiliary power supply ^f	P_{aps} (kW)	160
Efficiency of auxiliary power ^f	η_{laps} (-)	0.95
Proportion of regenerated energy ^g	P_{reg} (-)	0.95

^aIntercity configuration (TRM1 - 472 seats; TRM2 - 696 seats) (TKTA, 2008);

^bTRM 08;

^cThe maximum speed is up to 500 km/h (TKTA, 2008);

^dInter-city configuration/composition (TRM08); Thornton, 2009 (Including effects of length);

^eNot relevant due to providing stability of the vehicle/train;

^fZiemke (2010);

^gUSDT (2004).

Table 3. Input data - HL (Hyperloop).

Characteristic/variable/parameter	Notation/dimension	Value
Carriages per vehicle/train ^a	–	1
Length	l (m)	32
Width	w (m)	1.35
Height	H (m)	1.10
Frontal area of a vehicle/train	A (m ²)	1.4
Gross (total) mass ^a	m (tons)	15
Capacity ^a	PL (seats)	28
Load factor	λ (-)	1.0
Acceleration/deceleration (maximum) ^b	a^+/a^- (m/s ²)	1.0/1.5
Typical average cruising speed ^c	v_c (km/h)	1000
Maximum cruising speed ^a	$v_{c/max}$ (km/h)	1200
Speed at the moment of boost by LSM ^a	$v_{c/min}$ (km/h)	800
Number of boosts along the route ^d	n (-)	$S/\Delta s - 1$
Levitation height (vertical air gap)	h (mm)	1.5
Coefficient of the aerodynamic drag ^e	C_D (-)	0.328
Coefficient of the aerodynamic lift ^f	C_L (-)	0.0
Radius of tube ^f	R (m)	1.115
Longitudinal guideway angles ^g	$\theta_{ar}, \theta_{cr}, \theta_d$ (°)	0.06
Air density (tube) ^g	ρ (kg/m ³)	0.0008
Difference of the pressure in tube(s) ^g	$\Delta p = p_l - p_r$ (bar)	0.030
Power of the compressor system onboard ^h	P_{cs} (kW)	$P_{cs} = 140 (v/c) + 247; R^2 = 1$
Overall efficiency of the traction system ⁱ	η_w (-)	0.80
Efficiency of the vacuum pumps ^j	η_{vp} (-)	0.85
Time of maintaining vacuum in tube(s)	$\Delta \tau$ (h)	1–1.25

^aChin et al. (2015); Musk (2013); Taylor et al. (2016);

^bHigher than that of the HSR, TRM, and commercial aircraft;

^cAs an average due to the periodic boosting by LSMs;

^d Δs is the distance between location of LSMs in the tube;

^eAngle of attack: $\alpha = 0^\circ$ ($C_D = 2.1201 \cdot M^2 - 2.4069 \cdot M + 0.7169$; $R^2 = 0.9672$; M is Mach number; Decker et al., 2017);

^fNot relevant due to operating in the almost vacuumed tube including the requirement for the vehicle/train stability;

^gMusk (2013);

^hDifference between the medium and the ultra-high vacuum recovered due to eventual leakage from the tube;

ⁱChin et al. (2015);

^jDecker et al. (2017).

seats) (Boeing 737-800) (Case b). The APT aircraft are considered to operate at the short- to medium-haul nonstop journey distances of $S = 400$ – $1,200$ km.

5.2. Analysis of the results

The results of the application of the models are shown on Figures 7(a, b), 8, 9, 10(a, b), & 11. Figure 7(a, b) shows the

Table 4 Input data - APT (Air Passenger Transport).

Characteristic/variable/parameter	Notation/Dimension	Aircraft type	
		B373-800 ^a	CRJ1 - 700 ^b
Capacity ^c	PL (seats)	189	50
Maximum TOW (Take-of-Weight) ^c	m (tons)	65.3	21
Load factor	λ (-)	1.0	1.0
Average climb/descent rate ^d	R_{CD} (ft/min)	1770/2000	1770/2000
Cruising altitude ^c	H (10^3 ft)	31	31
Climb/descent time ^d	$\tau_{R/C}$ min	17.5/13.0	17.5/13.0
Typical cruising speed (TAS) ^c	v_c km/h	823	823
Average fuel consumption – climbing ^d	FC_{cl} (kg/min)	95.3	32.4
Average fuel consumption - cruising ^d	FC_{cr} (kg/min)	44.1	19.2
Average fuel consumption – descending ^d	FC_{de} (kg/min)	7.1	6.0
Average fuel consumption - LTO cycle ^e	FC_{LTO} (kg/LTO)	880	330
Energy content of Jet A fuel ^f	MJ/kg	42.8	42.8

^aBoeing;^bCanadair Regional Jet;^cEEC (2004, 2009); Park and O'Kelly (2014) (TAS -True Air Speed; ft - feet; 1 ft = 0.305 m);^dCompiled from EEC (2004, 2009);^eLTO (Landing and Take-Off) cycle; ICAO (2011);^fMJ - Mega Joule (1 MJ = 0.27778 kWh).

relationship between the average energy consumption and the nonstop journey distance for the three HS rail-based systems.

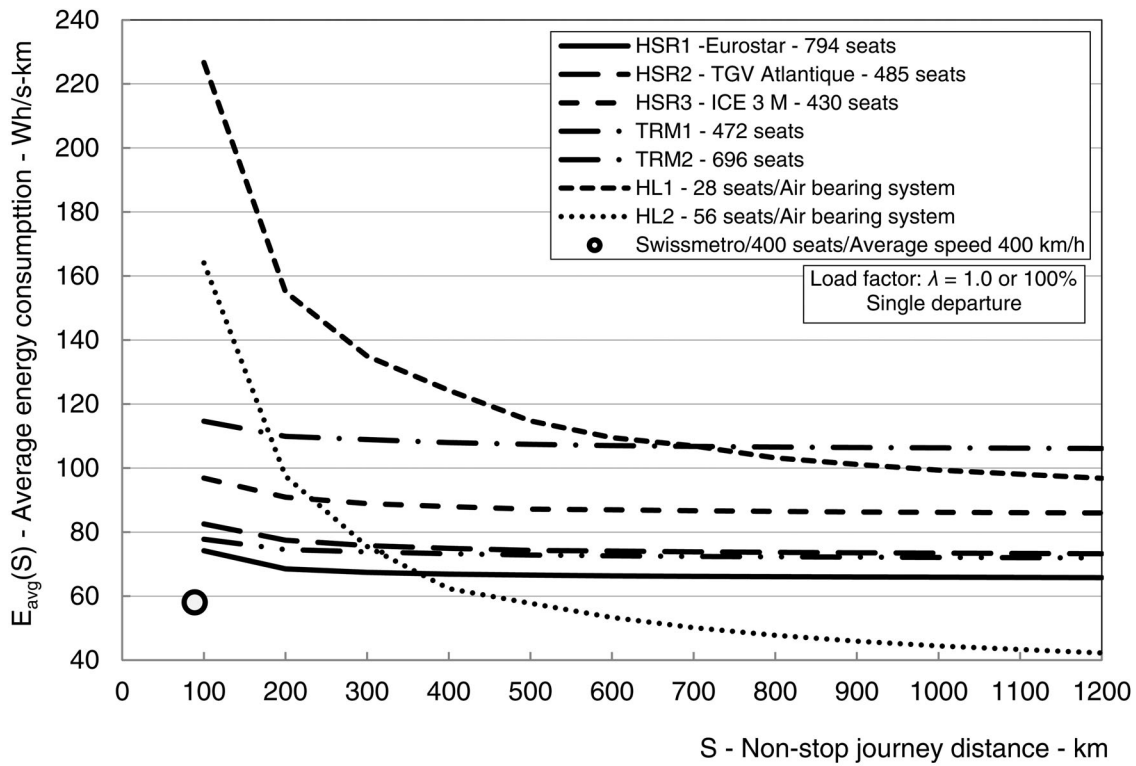
Figure 7(a) shows that the average energy consumption per departure of the three systems decreases more than proportionally with the increase of the nonstop journey distance and their seating capacity. In the case of the HSR and the TRM the influence of distance was relatively modest compared to that of the seating capacity. The average energy consumption of the HSR1 (Eurostar – 794 seats) was lower than that of the HSR2 (TGV Atlantique – 485 seats) and the HSR3 (ICE 3M – 430 seats) vehicle/train configuration. One of the influencing factors was the weight-to-seat ratio of 0.974 for the Eurostar, 0.988 for the TGV Atlantique, and 1.016 for the ICE 3M vehicle/train. The average energy consumption of the TRM2 (696 seats) was lowered by about 57% compared to the TRM1 (472 seats) vehicle/train configuration. In the case of the HL system, the influence of journey distance and seating capacity on the average energy consumption was much greater than that of its two counterparts. Compared to those of the HSR and the TRM, the energy consumption of the HL1 (28 seats) and the HL2 (56 seats) vehicle/train configuration decreases at the highest rate with the increase of the nonstop journey distance. At the same time that of the HL1 was about 50% higher than that of the HL2 vehicle/train configuration. In addition, the average energy consumption of the HSR1 (794 seats) was for about 7% and 37% lower, respectively, than that of the TRM2 and the TRM1 vehicle/train configurations. However, this energy consumption of the TRM1 was about 43% and 22% higher than that of the HSR2 and the HSR3 vehicle/train configurations, respectively. That of the TRM2 was lower about 3% and 18%, respectively, compared to the HSR2 and the HSR3 vehicle/train configurations. On the journey of distances between 500 and 1,200 km, the average energy consumption of the HL1 was about 2, 1.9, and 1.6 times higher, respectively, than that

of the HSR1, the HSR2, and the HSR3 vehicle/train configurations. In addition, that of the HL2 was lower about 25%, 32%, and 42%, respectively, than that of the HSR1, the HSR2, and the HSR3 vehicle/train configurations. This energy consumption of HL1 was higher than that of the TRM1 vehicle/train configuration by about 20% at distances up to 700–800 km, and become increasingly lower beyond them. As well, it was higher than that of the TRM2 by about 1.9 times. At the same time, the energy consumption of the HL2 was increasingly lower than that of the TRM1 and the TRM2 vehicle/train configuration beyond distances of about 300 km.

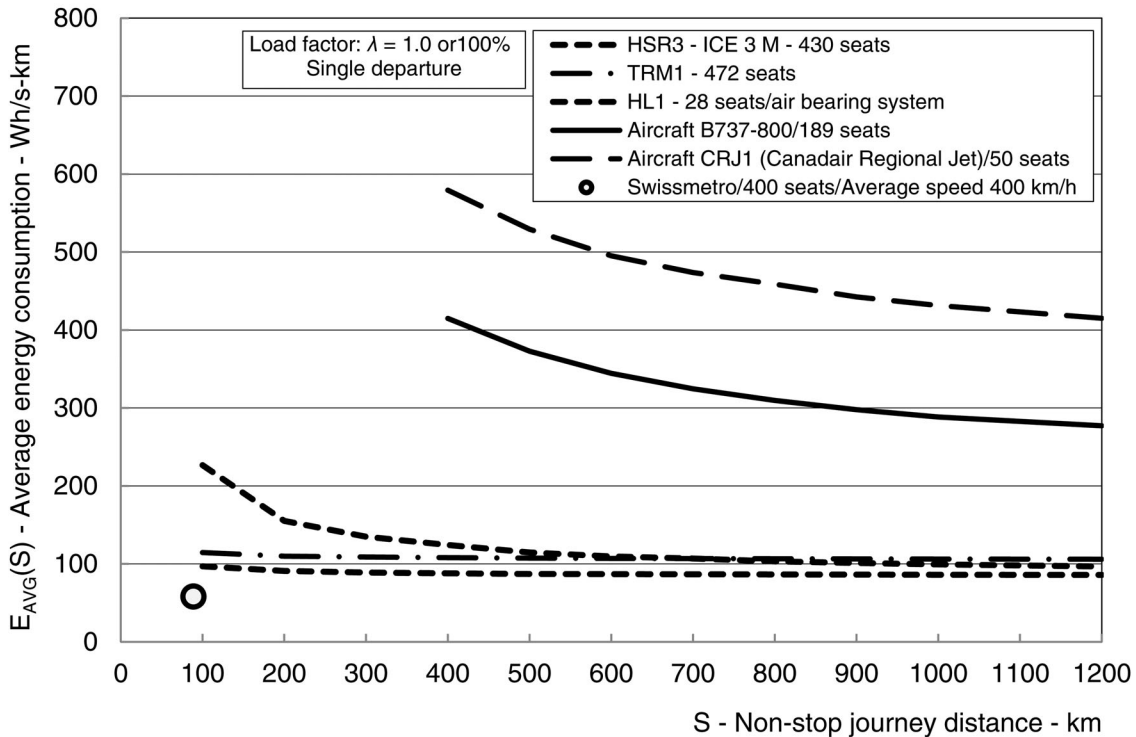
Figure 7(b) shows that three HS rail-based systems had lower energy consumption than two APT aircraft operating on the given journey distance(s). In addition, for both aircraft types, the energy consumption decreased with the increase in the journey distance, at decreasing rate (about 0.30–0.37), which was lower than that of the HL but higher than that of the HSR and the TRM vehicle/train configuration. In addition, Figure 7(a, b) shows that the average energy consumption of the Swissmetro operating on the average nonstop distance of 100 km would be lower than that of the above-considered four systems (Cassat et al., 2003).

Figure 8 shows the average CO₂ emissions by the three HS systems operating in the above/mentioned vehicle/train configurations and the APT system operating two aircraft types on two distances, $S = 500$ and $S = 1,000$ km.

As can be seen, the corresponding CO₂ emissions (per departure) have also changed proportionally to the change in energy consumption, depending on the journey distance. At both distances, the HL2 (56 seats) scored the best, followed by that of the TRM2 (696 seats) and the HSR1 (794 seats) vehicle/train configuration. In addition, CO₂ emissions by the TRM1 (472 seats) have been comparable to those of the HL1 (28 seats) vehicle/train configuration. These were all lower than both the APT aircraft types.



a) HSR, TRM, HL



b) HSR, TRM, HL, APT

Figure 7. Relationship between the average energy consumption and the nonstop journey distance of the considered HS transport systems. a) HSR, TRM, HL b) HSR, TRM, HL, APT.

Figure 9 shows the relationships between the total energy consumption and the journey distance of the three HS rail-based vehicles/trains and the APT aircraft with the capacity

of 189 seats. These are estimated for single departure (Case a) and if the single departure of the HSR, the TRM and the APT were to be replaced by the equivalent number of

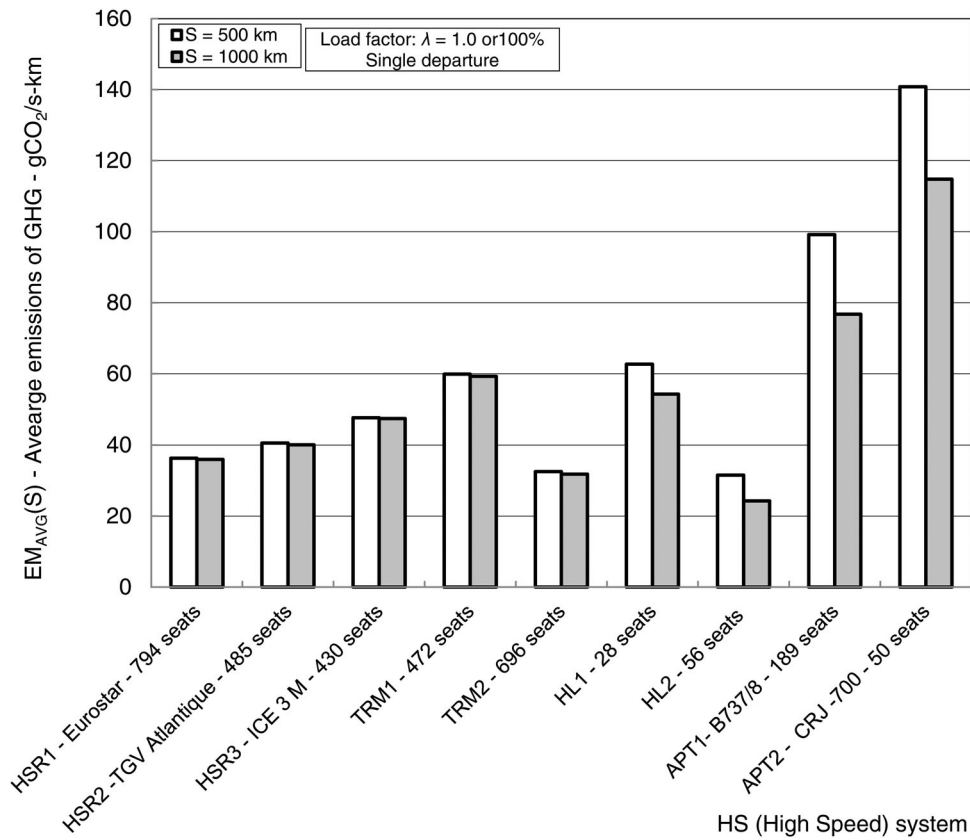


Figure 8. Relationship between the average CO₂ emission and the nonstop journey distance of the considered HS transport systems.

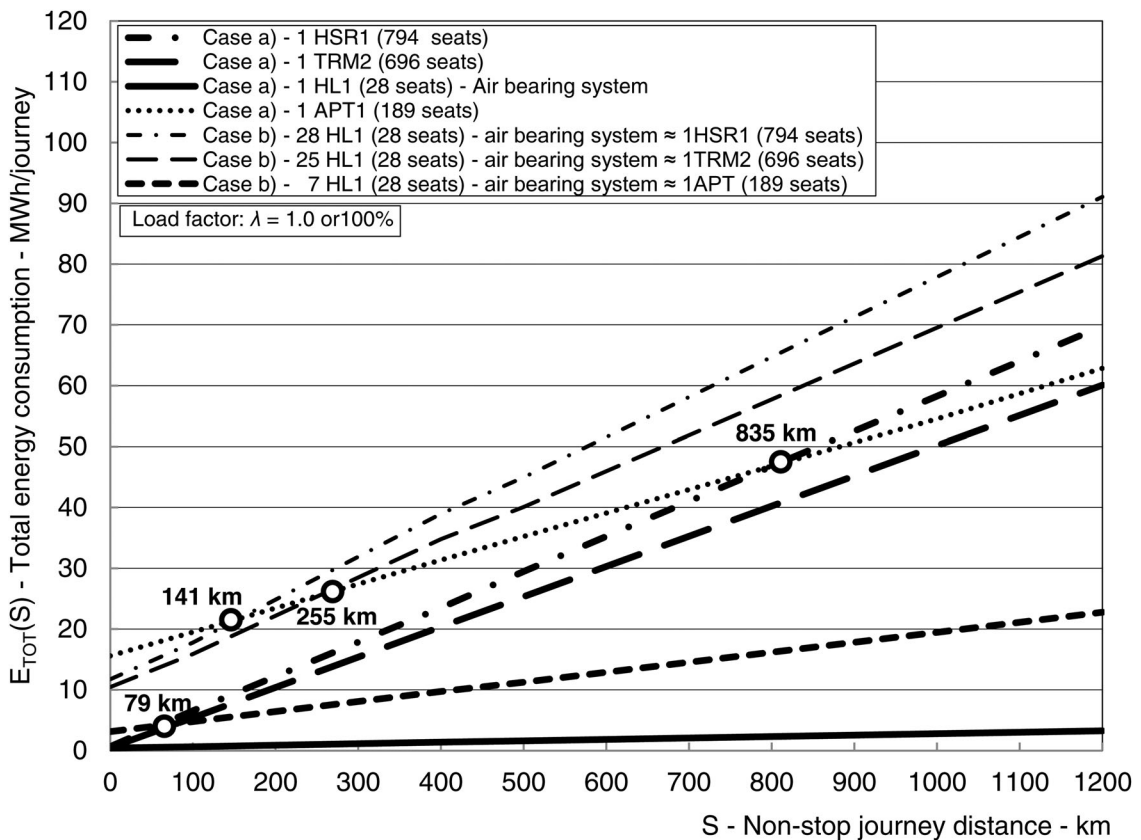
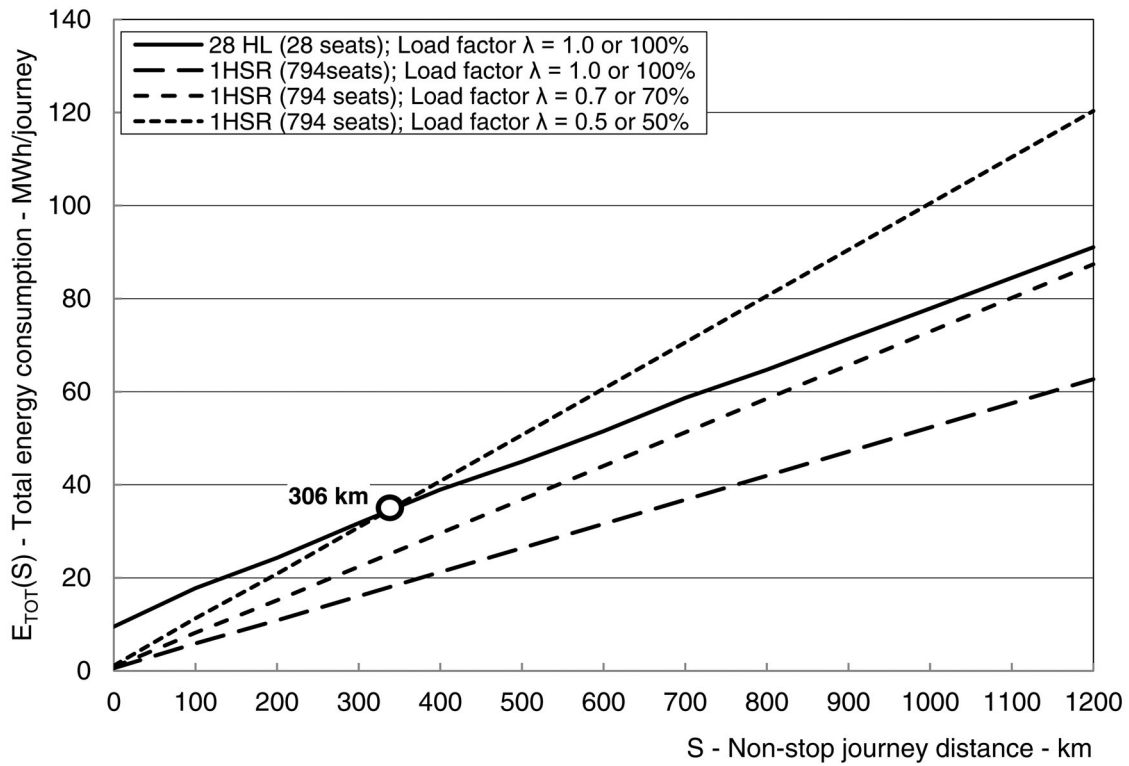
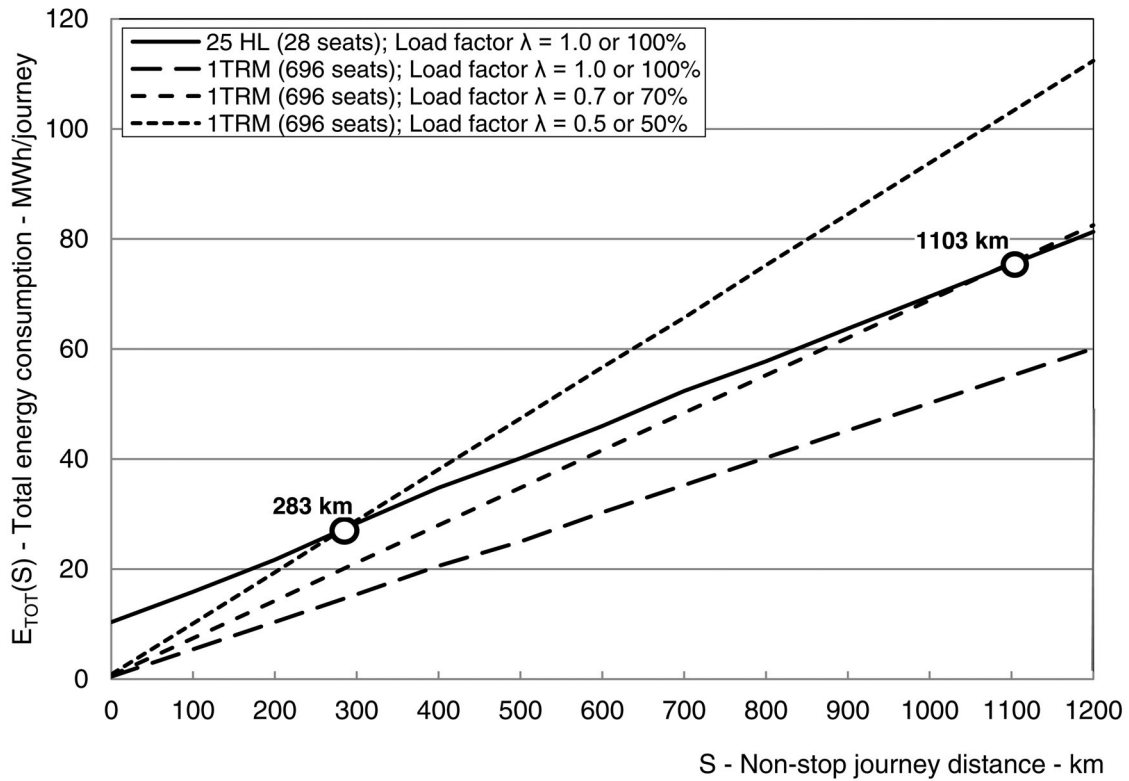


Figure 9. Relationship between the total energy consumption and the nonstop journey distance of the considered HS transport systems (Equivalent transport capacity (seats)).



a) 28 HL (28 seats) vs 1 HSR (794 seats)



b) 25 HL (28 seats) vs 1 TRM (696 seats)

Figure 10. Relationship between the average energy consumption, vehicle/train load factor, and journey distance of the considered HS transport systems. a) 28 HL1 (28 seats) vs 1 HSR1 (794 seats) b) 25 HL1 (28 seats) vs 1 TRM2 (696 seats).

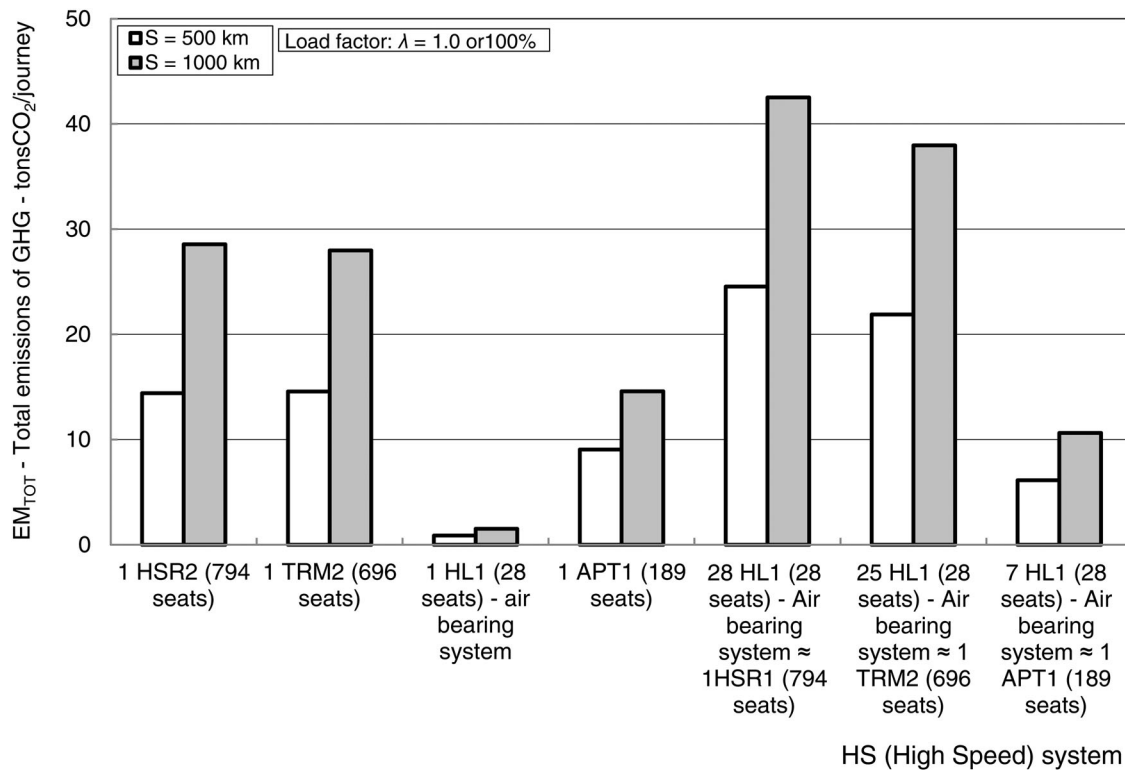


Figure 11. Relationship between the total CO₂ emissions and the nonstop journey distance of the considered HS transport systems (Equivalent transport capacity (seats)).

departures and corresponding seating capacity of the HL vehicles/trains (Case b).

As can be seen, the total energy consumption of the vehicle/trains of all systems linearly increases with the increase of the journey distance. In Case a) the total energy consumption was the highest for the HSR1, followed by that of the TRM2, and the lowest for the HL1 vehicle/train configuration. The gap between the total energy consumptions of these vehicles/trains increases with the increase of the journey distance. In addition, the energy consumption of APT aircraft, which is the highest at shorter distances, becomes lower than that of the HSR1 vehicle/train configuration beyond a distance of 835 km. In addition, the energy consumption of an APT departure becomes lower than that of 25 HL1 (Equivalent to 1 TRM2) and 28 HL1 (equivalent to 1 HSR1) departures beyond a distance of 255 km and 141 km, respectively. The energy consumption of 7 HL1 vehicle/train departures (equivalent to 1 APT departure) becomes lower than that of the single departure of the HSR1 and the TRM2 vehicle/train configuration beyond a distance of about 79 km.

As well under conditions of providing the equivalent transport capacities, 25 HL1 vehicle/train departures would consume for about 2.93 ($S=100$ km) and 1.35 ($S=1,200$ km) times more energy than their single TRM2 vehicle/train equivalent. At the same time, 28 such HL1 vehicle/train departures would consume for about 2.71 ($S=100$ km) and 1.30 ($S=120$ km) times more energy than their single HSR1 vehicle/train counterpart, and 7 HL1 vehicle/train departures would consume for about 3.21

($S=400$ km) and 2.80 ($S=1,200$ km) times less energy than their single APT aircraft counterpart.

Figure 10(a, b) shows the relationship between the average energy consumption, the vehicles/train load factor, and the nonstop journey distance of the three HS systems supplying the equivalent seating capacities along the line/route.

Figure 10(a) shows that the positive difference between the total energy consumption of the HSR and the HL vehicle/train decreases with the decrease of the load factor of the HSR vehicle/train (the load factor of HL vehicles/trains remains 100%). For example, if the load factor is decreased to 70% and 50%, the energy consumption of a single HSR vehicle/train departure would increase and become higher so that its HL counterparts beyond the nonstop journey distance are about 1,200 km and 306 km, respectively. Figure 10(b) shows that the difference between the total energy consumption of the TRM2 and the HL1 again increases with the decrease of the load factor of the TRM2 vehicle/train (that of HL vehicles/trains remains 100%). For example, if the load factor is decreased to 70% and 50%, the energy consumption of the TRM2 vehicle/train would increase and become higher, equivalent to that of HL1 vehicles/trains beyond a distance of about 1,100 km and 283 km, respectively. These examples indicate that decreasing of load factor generally contributes to the increase of fuel consumption, under conditions of supplying equivalent transport capacities. This happens despite the decreases of the gross weight of vehicles/trains due to the decrease of the payload weight, i.e. the number of passengers onboard. Further analysis of the total demand and its share

among the three systems could contribute to a more precise estimate of their load factors and the break-even distances regarding energy consumption.

In addition, Figures 9 and 10(a, b) show that the considered systems also consume energy at the journey distance $S=0$. In the case of the HSR system, energy is consumed for the limited re-positioning, lighting, air conditioning, and providing other amenities for trains during passenger disembarking and embarking and carrying out supporting operations at the rail terminals. In the case of the TRM and the HL, in addition to the same operations as in the case of the HSR system, energy is consumed for initially setting up the levitation force before running the line/route. The related energy consumption of APT aircraft is much higher than that of its three rail-based counterparts. This is due to the fuel consumption of aircraft engines during the LTO cycle and the Auxiliary Power Unit (APU) operating in parallel during arrival, departure, and single (at the gate) cycle (Liu et al., 2016; Padhra, 2018).

Figure 11 shows the corresponding total CO₂ emission for the selected journey distances operated by the three HS rail-based vehicles/trains and the APT aircraft with the given seating capacity. The values for the single departure of the HSR1, the TRM2, the HL1 vehicle/train and the APT1 aircraft configuration (Case a), and when the HSR1, the TRM2 vehicle/train and the APT1 aircraft is replaced by the equivalent seating capacity of HL1 vehicles/trains (Case b) have been estimated.

As can be seen, analogously to the total energy consumption, in Case a) the total CO₂ emission by the HSR1 is the highest and comparable to that of the TRM2 vehicle/train configuration. The value for the HL1 vehicle/train has been the lowest. The APT1 aircraft has a lower value than those of the HSR1 and the TRM2 vehicles/trains. This has been due to differences in CO₂ emission rates (0.266 vs 0.546 kgCO₂/kWh) and the lower average energy consumption of the latter two. In Case b) the total CO₂ emission of the 28 HL1 vehicles/trains replacing the single departure of the HSR1 vehicle/train is the highest. This is followed by that of the 25 HL1 vehicles/trains replacing a single departure of the TRM2 vehicle/train, and 7 HL1 vehicles/trains replacing a single APT1 departure. In both cases, as expected, the total CO₂ emission of all the systems increases with the increase of the nonstop journey distance.

6. Conclusions

This paper has presented an approach to direct estimation of energy consumption and related CO₂ emission of three High Speed (HS) rail-based passenger transport systems: High Speed Rail (HSR), TransRapid Maglev (TRM), and Hyperloop (HL). This includes the development of the corresponding analytical models, based on the mechanical energy of the operating vehicles/trains and their application, according to what-if operating scenarios. These models have a simplified structure due to not including details of the behavior of the electric systems of vehicles/trains. The what-if operating scenarios implied carrying out nonstop journeys

along a straight line/route, without considering details of the driving processes. The energy consumption and CO₂ emission by Air Passenger Transport (APT) aircraft operating in line with a comparable what-if scenario have been provided for comparative purposes.

6.1. Results from application of the models

The results of the application of the proposed models indicate the following:

- The average energy consumption and related CO₂ emission per departure of the vehicle/train of either capacity operated by the three ground HS rail-based systems and their APT aircraft counterpart generally decrease more than proportionally with the increase of the nonstop journey distance. They also decrease with the increase of the seating capacity per departure, in the case of all four considered systems, independently of the nonstop journey distance.
- The HSR vehicle/train with the highest seating capacity has a lower average energy consumption and related CO₂ emission than the TRM vehicle/train of higher, and HSR and TRM vehicle/train of lower seating capacity. The HL vehicle/train with the original seating capacity has been several times less efficient than its counterparts. The HL vehicle/train with double seating capacity could be more efficient than its HSR, TRM, and APT counterparts only beyond a 'critical' journey distance.
- The total energy consumption and related CO₂ emission per single departure of the vehicles/trains of the three rail-based systems and selected APT aircraft increase linearly with the increase of the nonstop journey distance. In the case of the HL vehicle/train departure the values are lower than those of the TRM and the HSR vehicle/train, and the APT aircraft, respectively, independent of the journey distance. When providing the equivalent seating capacities per departure, the total energy consumption and related CO₂ emission are highest for the HL vehicle/train departures replacing the single departure of the HS and the TRM vehicle/train with the highest seating capacity, respectively, independently on the journey distance.

The presented approach for estimating the direct energy consumption and CO₂ emission, their comparison between the different HS rail-based passenger transport systems, and the obtained results have been limited by the abovementioned rather simplified analytical models, the specified what-if operating scenarios, and the availability of reliable input data.

Nevertheless, these analytical models and their results have sufficiently reflected the essential characteristics of the three rail-based HS systems in the given context, despite not including their driving processes and behavior of the electrical systems in detail. Consequently, they could be used for indicating directions and space for more detailed further research, as follows:

- Extending the scope of consideration of the energy consumption and related CO₂ emission, from the current direct-operations to the Life Cycle Assessment (LCA) approach; this should also include other Green House Gases (GHG);
- Finding the way for collecting more reliable, sufficient, and detailed data, not only from secondary sources but also from forthcoming TRM and HL projects and experiments;
- Developing more detailed models of the energy consumption and CO₂ emission of the three HS rail-based passenger transport systems, by including the driving processes and behavior of the electric systems of vehicle/trains operating according to more realistic traffic scenarios;
- Considering the three HS rail-based passenger transport systems operating in the networks of lines/routes, including their mutual relationships through exclusivity, complementarity, or competition;
- Including other performances for the comparison of the three HS rail-based passenger transport systems, defining the corresponding indicators, and developing models for their estimation; and
- Applying Cost-Benefit-Analysis (CBA) and/or multi-criteria evaluation methods for assessing the overall social-economic feasibility of these HS rail-based passenger transport systems, based on their market potential and the total costs of implementation and operation.

6.2. Some implications and policy recommendations

The estimated energy consumption and CO₂ emission of the three HS rail-based transport systems (HSR, TRM, and HL), extended by their LCAs, would be particularly relevant in elaborating policies aimed at developing a more sustainable integrated HS transport system. Such a system would generally continuously increase its overall social-economic benefits while at the same time contributing to mitigating environmental and social impacts. The main impacts would be reducing total energy consumption and related GHG emission. This would be achieved by implementing the most energy efficient system(s), using the primary sources for obtaining electric energy with a minimal or no CO₂ emission. Solar, wind, and nuclear primary sources could be considered. Improving engine and aerodynamic efficiency and introducing partially low-carbon alternative fuels for APT aircraft would contribute to marginally reducing fuel consumption and emission of GHG, including CO₂. More general aspects of sustainability policy in the given context would relate to: i) motivation; ii) economic costs; iii) effects/impacts on mobility; iv) environmental advantages; and v) economic and regional effects/impacts.

6.2.1. Motivation

The motivation behind the implementation of the HL or the TRM system is expected to be country specific. In general, similarly as the HSR and the APT, the TRM and the HL

system would aim to reduce (i.e. save) travel time and consequently increase technical productivity, thanks to higher operating speeds. The primary issues relevant for policy makers would be their potential contribution to regional social-economic development. This can also influence the spatial configuration of the HL and/or TRM networks, either connecting the given country's capital to peripheral cities or directly connecting all main cities. An additional issue would be the market position and influence of the HL or the TRM systems, exclusively complementing or competing with the HSR and/the APT.

6.2.2. Costs

Similar to the HSR, the HL and the TRM systems would entail high investment costs, which would mainly depend on length of the particular links and network. These investments, operating, environmental, and social costs, and the prospective benefits/revenues need to be evaluated in order to assess whether the particular HL and TRM projects would be overall economically-socially profitable/feasible. The CBA could be one of the suitable evaluation methods.

6.2.3. Effects/impacts on mobility

The TRM or HL system, implemented in a given corridor, could generally have two effects/impacts on existing mobility. First, it could generate additional/new passenger demand. Second, it could attract passengers from existing modes – generally from the HSR, the APT, conventional rail, and road. Therefore, the consequent changes of the modal/system market shares could also be a relevant policy issue.

6.2.4. Environmental and social advantages

The lower energy consumption and CO₂ emission, along with some short- to medium-haul distances, indicate that the HL and/or the TRM could eventually be sufficiently environmentally and socially efficient compared, to the HSR and the APT system. Their efficiency regarding land use and related impacts during implementation, needs to be especially considered. The related effects and impacts should be evaluated in the scope of the system's overall socioeconomic feasibility.

6.2.5. Economic and regional effects/impacts

Interesting and important policy issues relate to the indirect economic and regional effects of the new systems, such as the HL or the TRM. The former would be the system's ability to generate sufficient economic activity and related employment. Would it stimulate spatial cohesion and work productivity across the area/territory it serves? Or would it contribute to achieve the opposite, i.e. the spatial dispersion of the particular existing and new businesses? Therefore, the recommended policy issue would be to investigate the system's potential balance between increasing inter-territorial cohesion and territorial polarization. An additional policy issue would be if the presumably improved accessibility of

the cities connected by the HL or the TRM system networks could be more beneficial than the compromised transport services of the existing/competing transport modes and their systems. Also, the policy recommendation would relate to investigating the influence of the TRM and the HL systems on the specific activities. For example, on the one hand their high speed could benefit business passengers in general, while on the other, it could shorten the passengers' stay at destinations and consequently affect the tourist industry and related services.

References

- Agora Energiewende and Sandbag. (2018). *The European power sector in 2017: State of affairs and review of current developments*. www.sandbag.org.uk
- Baker, C. (2014). A review of train aerodynamics part 2-applications. *The Aeronautical Journal*, 118(1202), 345–382. <https://doi.org/10.1017/S0001924000009179>
- Campos, J., & de Rus, G. (2009). Some stylized facts about high-speed rail: A review of HSR experiences around the world. *Transport Policy*, 16(1), 19–28. <https://doi.org/10.1016/j.tranpol.2009.02.008>
- Cassat, A., Bourquin, V., Mossi, M., Badoux, M., Vernez, D., Jufer, M., Macabrey, N., & Rossel, P. (2003). *Swissmetro: Project development status*. International Symposium on Speed-up and Service Technology for Railway and Maglev Systems 2003 (STECH '03) (pp. 19–22). Transportation and Logistics Division, Japan Society of Mechanical Engineering (JSME).
- Cassat, A., & Bourquin, V. (2011, Décembre 14–15). *MAGLEV - Worldwide status and technical review*. Électrotechnique du Futur.
- Chin, J., Gray, J., Jones, S., & Berton, J. (2015, January 5–9). *Open-source conceptual sizing model of the hyperloop passenger pod* [Paper presentation]. 56th AIAA/ASCE/AHS/ASC Structures, Structural Dynamics, and Materials Conference, Kissimmee, Florida, USA. <https://doi.org/10.2514/6.2015-1587>
- Davis, W. J. Jr., (1926). Tractive resistance of electric locomotives and cars. *General/Electric Review*, 29, 685–708.
- Decker, K., Chin, J., Peng, A., Summers, C., Nguyen, G., Oberlander, A., Sakib, G., Sharifrazi, N., Heath, C., Gray, S. J., & Falck, R. (2017, January 9–13). *Conceptual feasibility study of the hyperloop vehicle for next-generation transport* [Paper presentation]. Scientific Technology Conference, Grapevine, Texas, USA.
- EC. (1996). *Interoperability of the trans-European high speed rail system, Directive 96/48/EC*. European Commission.
- EEC. (2004). *Aircraft performance summary tables for the Base of Aircraft Data (BADA)* (EEC note No. 12/04). EUROCONTROL.
- EEC. (2009). *Base of Aircraft Data (BADA): Aircraft performance modelling report* (EEC Technical/Scientific Report No. 2009-009). EUROCONTROL.
- EPFL. (1993). *Swissmetro: Synthèse Der Vorstudie* (EF Nr. 192 479). Ecole Polytechnique Federale de Lausanne.
- Feng, X., Sun, Q., & Li, M. (2014). Assessing energy consumption of high-speed trains based on mechanical energy. *Procedia - Social and Behavioural Sciences*, 138, 783–790. <https://doi.org/10.1016/j.sbspro.2014.07.260>
- Feigenbaum, B. (2013). High-speed rail in Europe and Asia: Lessons for the United States, Reason Foundation. *Policy Study*, 418, 1–39. www.reason.org
- Fritz, E., Klühspies, J., Kircher, R., Witt, M., & Blow, L. (2018). *Energy consumption of track-based high-speed transportation systems Maglev Technologies in comparison with steel-wheel-rail*. Research Series Volume 3. The International Maglev Board.
- Hwang, L. C., & Yoon, K. (1981). *Multi attribute decision-making: A methods and applications*. Lecture Series in Economics and Mathematical Systems. Springer-Verlag.
- ICAO. (2011). *Airport air quality manual* (1st ed.). Corrigendum No. 1, Doc 9889. International Civil Aviation Organization.
- Janić, M. (2003). Multiple criteria evaluation of high speed rail, TRANSRAPID MAGLEV and air passenger transport systems in Europe. *Transportation Planning and Technology*, 26, 491–512.
- Janić, M. (2014). *Advanced transport systems: Analysis, modelling, and evaluation of performances*. Springer.
- Janić, M. (2016). A multidimensional examination of the performances of HSR (High Speed Rail) systems. *Journal of Modern Transportation*, 24(1), 1–24. <https://doi.org/10.1007/s40534-015-0094-y>
- Janić, M. (2018). Multicriteria evaluation of the high speed rail, Transrapid Maglev and hyperloop systems. *Transportation Systems and Technology*, 4(4), 5–31.
- Janić, M. (2019). Future advanced long-haul evacuated tube transport (EET) system operated by TransRapid Maglev (TRM): A multidimensional examination of performance. *Transportation Planning and Technology*, 42(2), 130–151. <https://doi.org/10.1080/03081060.2019.1565161>
- Jong, J. C., & Chang, F. E. (2005). Models for estimating energy consumption of electric trains. *Journal of the Eastern Asia Society for Transportation Studies*, 6, 278–291.
- Kantrowitz, A. (1947). The formation and stability of normal shock waves in channel flows. National Advisory Committee for Aeronautics (Technical Note 1225). Langley Aeronautical Laboratory.
- Liu, H., Xu, Y. A., Stockwell, N., Rodgers, M. O., & Guensler, R. (2016). A comparative life-cycle energy and emissions analysis for intercity passenger transportation in the US by aviation, intercity bus, and automobile. *Transportation Research Part D: Transport and Environment*, 48, 267–283. <https://doi.org/10.1016/j.trd.2016.08.027>
- Magel, E. E. (2017). *A survey of wheel/rail friction*. National Research Council.
- Mossi, M., & Rossel, P. (2001, March 1–3). *Swissmetro: A revolution in the high-speed passenger transport system* [Paper presentation]. 1st Swiss Transport Research Conference (STRC), Ascona, Switzerland.
- Musk, E. (2013). *Hyperloop Alpha*. SpaceX. http://www.spacex.com/sites/spacex/files/hyperloop_alpha-20130812.pdf
- Padhra, A. (2018). Emissions from auxiliary power units and ground power units during intraday aircraft turnarounds at European airports. *Transportation Research Part D: Transport and Environment*, 63, 433–444. <https://doi.org/10.1016/j.trd.2018.06.015>
- Park, Y., & O'Kelly, E. M. (2014). Fuel burn rates of commercial passenger aircraft: Variation by seat configuration and stage distance. *Journal of Transport Geography*, 41, 137–147. <https://doi.org/10.1016/j.jtrangeo.2014.08.017>
- Peters, J.-L. (1983). Aerodynamics of very high speed trains and maglev vehicles: State of the art and future potential. *International Journal of Vehicle Design, Special Publications*, 3, 308–341.
- Rochard, P. B., Schmidt, F. (2000). A review of methods to measure and calculate train resistances. *Proceedings of the Institute of Mechanical Engineering Part F: Journal of Rail and Rapid Transit*, 214, 185–143.
- Schach, R., & Naumann, R. (2007). Comparison of high-speed transportation systems in special consideration of investment costs. *TRANSPORT*, 22(3), 139–147. <https://doi.org/10.3846/16484142.2007.9638116>
- Schetz, A. J. (2001). Aerodynamics of high-speed trains. *Annual Review of Fluid Mechanics*, 33(1), 371–414. <https://doi.org/10.1146/annurev.fluid.33.1.371>
- Socket, H. (1996). The aerodynamics of trains. In J.A. Schetz & A.E. Fuhs (Eds.), *Handbook of fluid dynamics and fluid machinery* (pp. 1721–1741). Wiley.
- Taylor, C. T., Hyde, D. J., & Barr, L. C. (2016). *Hyperloop commercial feasibility analysis: High level overview*. Volpe National Transportation research Centre, U.S. Department of Transportation.
- TKTA. (2008). *ThyssenKrupp Transrapid Australia submission in response to East West link needs assessment report "investing in transport"*. ThyssenKrupp Transrapid GmbH.
- UIC. (2010a). *High speed rail: Fast track to sustainable mobility*. International Union of Railways.

- UIC. (2010b). *High speed, energy consumption and emissions*. UIC Publications, International Union of Railways.
- USDE. (2016). *Environment baseline, Volume 1: Greenhouse gas emissions from the U.S. power sector*. Office of Energy Policy and Systems Analysis, U.S. Department of Energy.
- USDT. (2004). *Urban Maglev technology development program: Colorado Maglev project report technical memorandum*. Federal Transit Administration, U.S. Department of Transportation.
- Van Goeverden, K., Milakis, D., Janić, M., & Konings, R. (2018). Analysis and modelling of performances of the HL (Hyperloop) transport system. *European Transport Research Review*, 10(2), 1–17. <https://doi.org/10.1186/s12544-018-0312-x>
- Vuchic, R. V., & Casello, M. J. (2002). An evaluation of Maglev Technology and its comparison with high speed rail. *Transportation Quarterly*, 56, 33–49.
- Wang, C. X., & Sanders, L. (2012). Energy consumption and carbon footprint of high-speed rail projects: Using CAHSR and FHRS as examples. *Proceedings of the Institution of Mechanical Engineers, Part F: Journal of Rail and Rapid Transit*, 226(1), 26–35. <https://doi.org/10.1177/0954409711404641>
- Wendell, C., & Vranich, J. (2008). *The California high speed rail proposal: A due diligence report*. Reason Foundation (with Howard Jarvis Taxpayers Association and citizens against government waste).
- Wenk, M., Klühspies, J., Blow, L., Kircher, R., Fritz, E., Witt, M., & Hekler, M. (2018). Maglev: Science experiment or the future of transport? *Practical investigation of future perspectives and limitations of Maglev Technologies in comparison with steel-wheel-rail*. The International Maglev Board.
- Witt, M., & Herzberg, S. (2008). *Technical-economical system comparison of high speed railway systems*. Dornier Consulting GmbH.
- WNA. (2011). *Comparison of lifecycle greenhouse gas emissions of various electricity generation sources*. WNA Report World Nuclear Association.
- Zhou, J. (2014). *Improving the energy efficiency of high speed rail and life cycle comparison with other modes of transport* [PhD Thesis]. Imperial College London, Department of Mechanical Engineering.
- Ziemke, D. (2010). *Comparison of high-speed rail systems for the United States* [MSc Thesis]. Georgia Institute of Technology. <https://asia.nikkei.com/Business/Transportation/China-looks-to-build-new-maglev-rail-line-to-boost-economy>
- <https://www.businessinsider.nl/history-hyperloop-pneumatic-tubes-as-transportation-2017-8/?international=true&r=US/>
- <https://ec.europa.eu/eipp/desktop/en/projects/project-9401.html>
- http://www.railway-energy.org/static/Swissmetro_61.php
- <http://www.trainweb.org/tgvpages/tgvindex.html>
- <https://www.travelchinaguide.com/cityguides/shanghai/getting-around.htm/>
- <https://uic.org/High-Speed-History>
- https://en.wikipedia.org/wiki/Shanghai_maglev_train
- http://en.wikipedia.org/wiki/ICE_3